GEOLOGICA CARPATHICA, 2025, 76, 5, 313–336 https://doi.org/10.31577/GeolCarp.2025.11

Reinterpreting depositional environment of the Polish Outer Carpathian Menilite Beds: Tide, river and wave-influenced muddy shelf of the Lower Oligocene Dynów Marls

PIOTR S. DZIADZIO✉

Oil and Gas Institute – National Research Institute, Lubicz 25A Str., 31-503, Kraków, Poland

(Manuscript received February 20, 2025; accepted in revised form August 28, 2025; Associate Editor: Igor Broska)

Abstract: The Dynów Marls occur in the lower part of the Menilite Beds throughout the Carpathian Arc. These siliceous marls record decreasing salinity, anoxic bottom conditions, and pronounced endemism during the Lower Oligocene age (Nannozone NP 23), referred to as the Solenovian Event (loss of connection of the Paratethys with the world ocean). Until recently, these beds, and the rest of the Menilite Beds in the Outer Carpathians, were considered to be a product of deep-water sedimentation, rather than shallow-water sedimentation as interpreted, for example, in Austria and the Czech Republic. To explain this discrepancy, detailed sedimentological studies of the Dynów Marls were undertaken in the south-eastern part of the Silesian Nappe of the Polish Outer Carpathians, in three selected sections: A – in Gorlice; B – Zborowice; and C – Jabłonica Polska. Six facies are identified: F1 – Black mudstone (Menilite shale); F2 – Chert; F3 – Stratified marls; F4 – Sandy–pebbly marls; F5 – Marly-mudstone heterolithics; and F6 – Stratified and laminated sandstone. The facies are grouped into three facies associations that confirm deposition of the Dynów Marls in shallow-water rather than deepwater environments. Interpretation of the facies and their associations suggests conditions typical of a shallow lake or fresh to brackish shelf that was significantly influenced by tides and wave action. In addition to carbonate deposition, siliceous material was supplied by terrestrial rivers but partly produced in situ. Periodic tsunami-type events also occurred and can be traced over considerable distances. Section A at Gorlice provides clear evidence of a facies succession characteristic of deposition in shallow water. These facies exhibit cyclic repetitions that reflect fluctuations in relative sea level, i.e., in the depth of the shallow-water sedimentary basin. This interpretation is supported by the presence of tidal rhythmites, attributed to spring-neap tidal cycles. Moreover, the succession of facies across the Menilite Beds profile indicates both fluctuations in basin depth and a progressive deepening of the shallow shelf. A shallow deltaic system (Magdalena Sandstone), located above the Dynów Marls, has also been documented in this area. The proposed shallow-water interpretation of the study strata does not preclude the existence of deep-water deposits elsewhere in the Paratethys sedimentary basin during the Lower Oligocene. The evidence for tides in the studied lacustrine or shelf succession sections likely reflects the basin's connection to the open ocean in this area. The discovery and documentation of these shallow-water features mark an important advancement in understanding the paleoenvironmental evolution of the Carpathians. It also contributes significantly to knowledge of the depositional conditions of the Menilite Beds. The results support and refine previous interpretations and paleogeographic reconstructions.

Keywords: Carpathians, Menilite Beds, Dynów Marls, shallow water depositional environments, shallow-water shelf, tidal flat deposits, tsunamite

Introduction

The Dynów Marls (Dynów Member; Kotlarczyk 1966) are of particular interest in the Western and Central Paratethys (e.g., Kotlarczyk & Leśniak 1990; Schulz et al. 2004, 2005; Sachsenhofer et al. 2018; Jirman et al. 2019, 2020). They represent an outgrowth event associated with the isolation of the Paratethys from the world ocean and a decrease in salinity (12–14 %), anoxic conditions of the bottom sediment and strong endemism (with a uniform small-size (1–2 cm) of bivalves fauna) that occurred during the Lower Oligocene (calcareous nannoplankton Zone NP 23; Solenovian Event) (Rögl 1999; Schulz et al. 2004; Sachsenhofer et al. 2018).

✉ corresponding author: Piotr S. Dziadzio
dziadzio@inig.pl

Despite the large amount of data collected, studies conducted, and scientific articles published, the discussion on the sedimentary environment of these deposits is still ongoing (e.g., Kotlarczyk et al. 2006; Popov & Studencka 2015; Studencka et al. 2016; Jirman et al. 2019, 2020).

The debate concerns the interpretation of the depositional environment of the Dynów Marls, despite robust indicators based on geochemical studies, e.g., those developed for the Czech part of the Silesian Unit (Jirman et al. 2019), studies of endemic fauna (Popov & Studencka 2015; Studencka et al. 2016) in the Polish part of the Silesian Unit or of evident similarities with modern subaqueous muddy shelf deltas showing clear influence of waves and tides (Steel et al. 2024).

The discrepancy in interpretation concerns the assumed deep-water conditions of their deposition (e.g., Kotlarczyk et al. 2006; Górniak 2011; Czapkowicz 2012; Pastucha 2013; Studencka et al. 2016) as opposed to a shallow-water shelf setting (Dziadzio et al. 2016; Jirman et al. 2019; Dziadzio & Matyasik 2021). These may be due to the fact that they were studied in different tectonic units, with differing deposition conditions, of the Silesian or Skole, and which were originally located in different positions in the Carpathian basins. This paper presents the sedimentological characteristics of the Dynów Marls (siliceous marls) occurring in the succession of the Menilite Beds of the Polish part of the Silesian Unit (in three sections) and an interpretation of their depositional environment. The study provides the most complete sedimentary record to date of the Lower Oligocene sedimentary environment that had wave and tidal influence.

General geology

The study area is located in the Polish part of the Outer Carpathians (Fig. 1A and B), an accretionary prism traditionally divided into five tectono-lithofacial units called nappes (Koszarski et al. 1974; Książkiewicz 1975; Ślączka & Kaminski 1998), each of which comprises the fill of a separate basin with changing tectonic setting over time (e.g., Roca et al. 1995; Nemčok et al. 2000; Gągała et al. 2012).

From south to north, these are the Magura, Dukla, Silesian, Sub-Silesian and Skole units (Fig. 1B). However, the Carpathians should also be divided vertically (tectono-stratigraphically) into two units: (A) the lower (older), allochthonous Upper Cretaceous–Eocene accretionary prism, obducted from the basement as a result of subduction; (B) the upper (younger), Oligo–Miocene, para-autochthonous (wedge-top foreland basins) with Menilite and Krosno Beds deposited in a residual sedimentary basin, which prograded eastwards into present-day Ukraine (Dziadzio et al. 2019; Dziadzio & Matyasik 2021). The formation of the para-autochthonous is associated with the Paratethys Basin, usually dated to around the Eocene/Oligocene boundary, when a drop in sea level combined with the effects of the Alpine orogeny caused the separation and freshening of the Paratethys from the Mediterranean (Rögl 1999; Allen & Armstrong 2008).

Stratigraphic position of the Dynów Marls

The Dynów Marls lie within the Menilite Beds and are also known as the Dynów Member. Their stratotype was first described by Kotlarczyk (1966) from the Skole Unit. At its

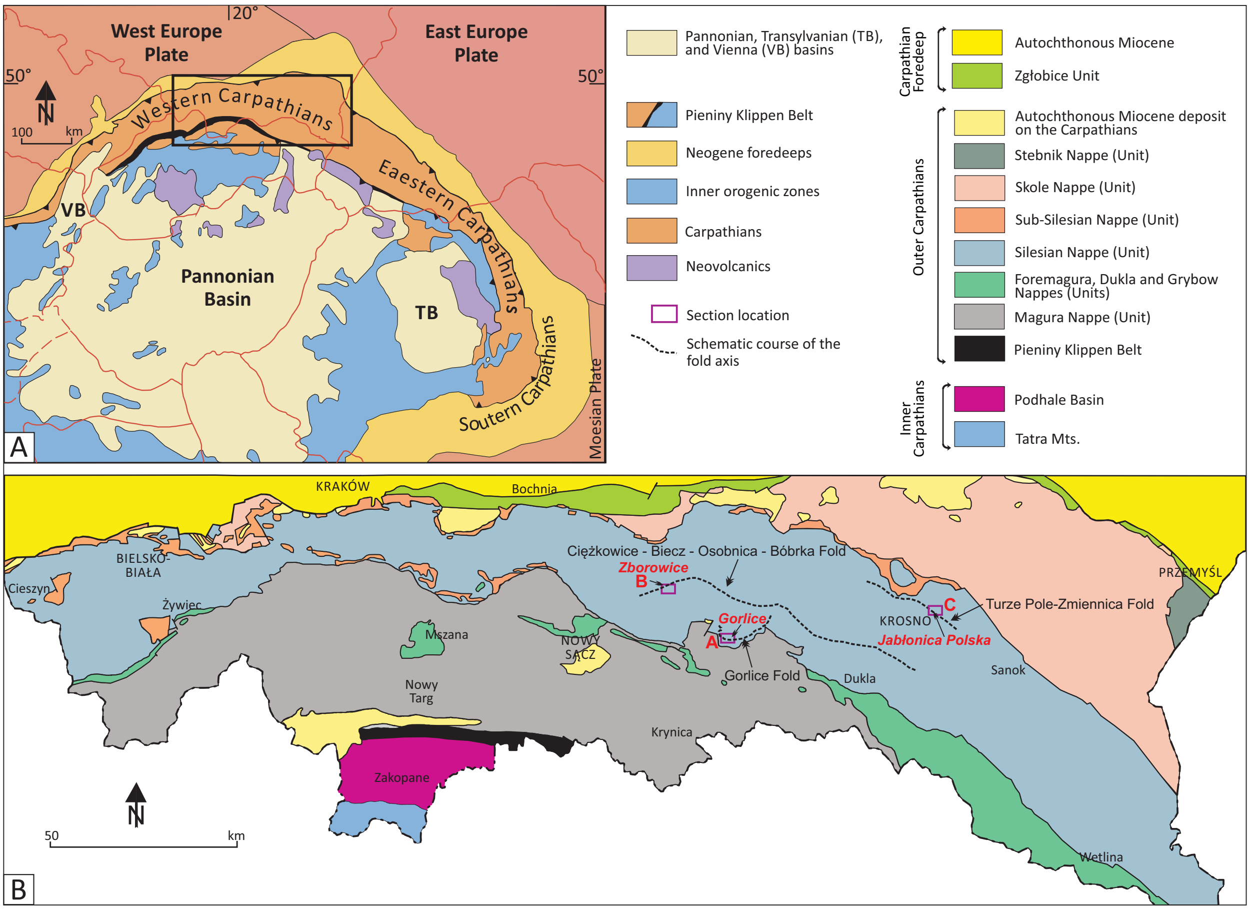

Fig. 1. A — General geological map of the Carpathians. **B** — Location of the investigated sections in the area of the Polish part of the Silesian Unit against the background of the geological structure of the Carpathians. Section A – Gorlice fold in the Sękówka riverbed in Gorlice), [49°38'51.77"N 21°10'41.58"E], Section B – Ciężkowice–Biecz–Osobnica–Bóbrka fold (in the Biała riverbed in Zborowice), [49°45'34.24"N 20°57'42.40"E] and Section C – Turze Pole–Zmiennica fold (in Jabłonica Polska), [49°42'39.96"N 21°54'6.43"E].

base are the Subchert Shale Member and the Kotów Cherts Member (Fig. 2). At the top there is the Rudawka Tractionites Member (with intercalations of the Tylawa Limestone) and other members within the Upper Menilite shale (Futoma Diatomite, Borek Nowy and Krępak Members; see: Kotlarczyk & Leśniak 1990; Kotlarczyk et al. 2006). They are assigned to the lowermost Rupelian (lower part of the NP23 nanoplankton zone, Fig. 2), (Kotlarczyk et al. 2006; Popov & Studencka 2015; Studencka et al. 2016).

In the Czech Republic, both the Silesian Unit (Jirman et al. 2019) and the Sub-Silesian Unit (Jirman et al. 2020), according to the results of stratigraphic studies, also correspond to the NP23 zone (Fig. 2). In the Silesian Unit, the Dynów Marls are underlain by the Subchert Member, and the Šitbořice Member is distinguished above the Dynów Marls (Jirman et al. 2019).

In Austria, the Dynów Marls occur in the Waschberg Unit in Lower Austria (a westward extension of the Ždanice Unit), as well as in the area of occurrence of the Upper Austrian Molasse Basin (Krhovský et al. 2001; Schulz et al. 2004). The equivalent of the Dynów Marls are also found in the Alpine Molasse area, the entire Carpathian Arc and the Transylvanian Basin (Krhovský 1981; Krhovský et al. 1992), and even from the Caspian Sea area, and are all related to the Solenovian Event and the isolation of the Paratethys from the world ocean (Rögl 1999; Krhovský et al. 2001; Schulz et al. 2004; Švábenická et al. 2007; Popov & Studencka 2015; Sachsenhofer et al. 2018; Jirman et al. 2019). For all three studied sections, the age of the Dynów Marls falls within the NP23 zone (Popov & Studencka 2015; Dziadzio et al. 2016; Studencka et al. 2016; Dziadzio 2018).

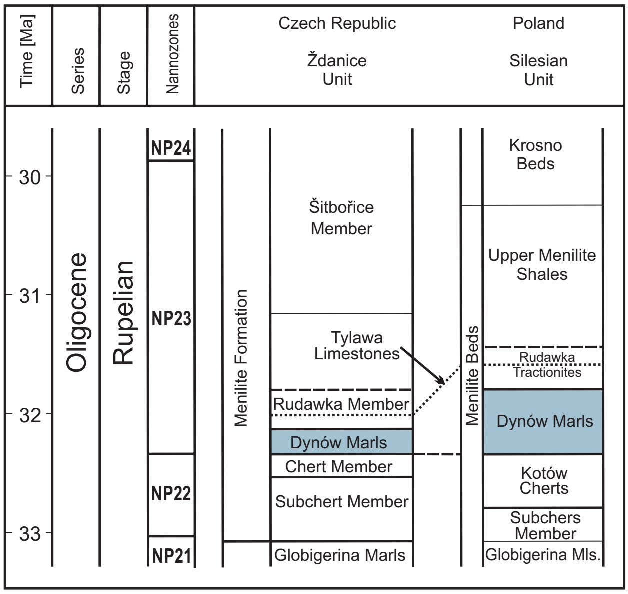

Fig. 2. Stratigraphic position of the Dynów Marls in Poland and the Czech Republic. Based on: Kotlarczyk et al. (2006); Studencka et al. (2016); Jirman et al. (2019) – modified.

Sedimentary environment of the Dynów Marls based on previous studies

The succession of Menilite Beds in the Polish part of the Outer Carpathians has been considered by many authors to be a product of deep-water sedimentation (e.g., Książkiewicz 1975; Unrug 1980; Kotlarczyk & Leśniak 1990; Kotlarczyk et al. 2006). However, based on recent studies (Schulz et al. 2004, 2005; Dziadzio et al. 2016, 2025; Jirman et al. 2019, 2020; Dziadzio & Matyasik 2021), this view should be reexamined.

Data from the tops and bottoms of many Dynów Marls successions in the Carpathian Arc (including those in Austria and the Czech Republic) provide marked evidence for shallow-water (shelfal water depth) conditions (Schulz et al. 2004, 2005; Jirman et al. 2019, 2020).

In Poland, both biostratigraphic data (calcareous nanoplankton), and geochemical data from section A suggest the sedimentary environment of the Dynów Marls should be defined as very shallow (shelf water depths), brackish (at the base) and very shallow, brackish with an eutrophic nature at the top (Dziadzio et al. 2016). The deposits most likely formed at times in an isolated lake-type basin, where laminated algal mats thrived (Dziadzio & Matyasik 2021). An alternative, as discussed below, is a delta-driven, fresh-water to brackish, hyperpycnal inner to mid shelf setting, to explain the marked sub-tidal rhythmites. The Dynów Marls in section C have also been interpreted in terms of the sedimentary environment, partly based on studies of calcareous nanoplankton and bivalves (Studencka et al. 2016). These conditions ranged from lacustrine (freshwater) to more stable marine conditions, with the average salinity of surface waters of mesohaline nature (Studencka et al. 2016). The described bivalve fauna is characteristic of the Solenovian Event, where mainly endemic taxa belonging to euryhaline bivalve families dominated. It should be noted that such salinity tolerance controls the zonal distribution of animals intidally influenced environments, with euryhaline species being particularly abundant in the supratidal zone (Newell 1979; Desjardins et al. 2012). At the same time, Studencka et al. (2016) write that the occurrence of Paleogene mollusc fauna in the Polish part of the Outer Carpathians is rare and limited to deep-sea sediments such asdebris flows or of olistoliths), similar to studies on fish (Kotlarczyk et al. 2006) and coprolites of teleost fish (Bajdek & Bieńkowska-Wasiluk 2020; Kotlarczyk & Leśniak 1990; Kotlarczyk et al. 2006; Studencka et al. 2016). There is therefore a basic disagreement as to whether the sediments reflect deep-water (bathyal) conditions or shallow-water conditions.

Materials and methods

The data for the study come from three measured sections of the Dynów Marls. They are located in the central-eastern Polish part of the Silesian Unit within three fold structures, (Fig. 1B).

All sections of the Dynów Marls were described from the sedimentological point of view and six main facies were distinguished within them (Table 1). For support of the interpretation twenty-nine samples were analysed for basic geochemistry from sections A, B and C using Rock-Eval-6 (nine samples each from sections A and B and 11 samples from section C). Thirteen detailed investigations of organic matter were also performed, including biomarker analyses using GC-MS Polaris Q (Thermo). Petrographic studies on six rock samples from sections B and C documented lithology, the main, secondary and accessory components, the degree of grain rounding, the occurrence of skeletal elements (and their degree of preservation), the type of cement and its genesis (primary or secondary), and diagenetic processes. These results were published by Dziadzio et al. (2025). To determine the stratigraphic position of the studied sections, data previously developed by Birecki (1964), Ślączka & Kaminski (1998), Dziadzio et al. (2016), Studencka et al. (2016), and Dziadzio (2018) were used.

Section A

Section A of the Dynów Marls (here called siliceous marls, Świdziński 1947) (Figs. 1B, 3, 4) is located in the lowest part of the Menilite Beds exposed on the southern limb of the Gorlice fold in the Sękówka riverbed. The thickness of the Menilite Beds here is about 150 to 200 m, though almost completely occupied by the coeval Magdalena Sandstone in this part of the Carpathians (e.g., Szymakowska 1979; Karnkowski 1999; Dziadzio et al. 2006, 2016; Dziadzio 2015a, b; Dziadzio & Matyasik 2021). The siliceous marl section is approximately 6.5 m thick, has not been described in detail and has not been identified previously as the Dynów Marls, except by Dziadzio & Matyasik (2021).

Section B

Section B is located in the lowest part of the Menilite Beds, in the Biała riverbed near Zborowice, on the southern limb of the Ciężkowice fold (Figs. 1B, 5). The thickness of the Menilite Beds is about 45 m and of the marls about 13 m (Fig. 5). However, Birecki (1964) distinguished a total of about 20 m of Menilite Beds and siliceous marls, dividing them into three levels: lower – subcherts, middle – cherts with accompanying marls, and upper – Menilite shales with lenses of Kliwa Sandstone. Such a tripartite division is not visible in the present section, which is now almost completely submerged. The author documented that in the upper part of the subchert beds there is a large quantity of well-preserved mollusc fauna and that in many places in the adjacent profiles within the Menilite Beds there are light, porous siliceous rocks – diatomites, which accompany the chert beds.

Section C

Section C is located in Jabłonica Polska on the southern limb of the Turze Pole–Zmiennica fold (Figs. 1B, 6, 7) and the Menilite Beds are about 8 to 70 m thick there (Wasiluk 2016). As described by Studencka et al. (2016), the Dynów Marls occur between the Kotów Cherts at the bottom and the Rudawka Tractionites with intercalations of the Tylawa Limestones at the top (Kotlarczyk et al. 2006). Near Jabłonica Polska, the marls are about 11 m thick (Fig. 7).

Results

Facies

Facies F1: Black mudstone (Menilite shale)

This facies (F1), (Table 1) is characterised by a clear shale separation when the mudstone fraction dominates, or a more massive texture without clear separation when the clay fraction dominates (Fig. 8). It contains little or no carbonate. However, it contains characteristic diverse and rather high amounts of organic matter (cf. Dziadzio et al. 2016, 2025) and notably lacks bioturbation.

Within this facies there are very thin layers, laminae or lenses (Fig. 8) of siltstones or very fine-grained sandstones that can have a horizontal, wavy (often symmetrical, Fig. 8) or lenticular lamination, showing continuity over a significant distance and allowing separation of the mudstone to occur at various thickness scales. This facies varies in colour from black to light brown, and on the weathered surface it ranges from white to light yellowish grey. A characteristic feature is the presence of sulphur efflorescences on the surface of the separation, which accentuate its yellow colour. The thickness of this facies varies from a few millimetres to several metres. It occurs together with facies F2, F3, and F5. Usually its contact with facies F3 is sharp (Figs. 3, 4, 5 and 8). This facies is widespread in the Lower Oligocene deposits of the Carpathian Arc.

Facies F2: Chert

Facies F2 (Table 1) occurs as isolated beds, several to 20 cm thick within facies F1, F3, F4 and as units several metres thick of parallel and wavy bedded cherts, often internally separated by very thin laminae of brown non-calcareous mudstones of facies F1 (Figs. 5 and 9). The cherts appear massive but can show subtle horizontal lamination, sometimes with additional primary sedimentary structures such as ripple cross-laminations, suggesting that they were originally siltstone and sandstones. The cherts are often interbedded with less silicified mudstones and weather to a pale yellowish-grey colour. Within the cherts, in addition to the Menilite shales, there are thin layers of sandstone, often lenticular in shape, both more siliceous and more like sandy mudstones. Their internal laminations are distinctly symmetrical ripples. These structures are clearly visible in the lower interval of section C, classified as the Kotów Cherts (Figs. 6 and 7).

Table 1: Summary of facies types observed in the Dynów Marls.

Facies	Lithology	Texture/structure/colour/other	Sedimentary structures/other	Thickness/type of bed contacts/geometry	Deposition processes	Sedimentary environment	Occurrence within the FA
F1. Black mudstone (Menilite shale)	**Mudstone, claystone**	Fine-grained (silty, clayey)/ massive, sally, flaky, thinly bedded/brown, black/large and variable amounts of organic matter	None, subtle horizontal lamination, wavy symmetrical, silt and very fine-grained sandstone laminae	From a few millimetres (beds) to several metres (packages)/ sharp tops and bottoms/tabular with high lateral continuity, lenticular	Hypopycnal suspension, combined or oscillatory flows or deposition as a result of intrabasinal gravity waves	Isolated shallow-water (lacustrine or freshwater inner shelf), above the storm wave base, in periodically isolated areas (bays, estuaries, lagoons, coastal lakes)	FAI, II, III
F2. Chert	**Chert**	Structureless, cryptocristaline/ massive, bedded/light brown to black/ rock breaks into cube-like fragments	None/thin streaks highlighted by colour change (in microscale) horizontal, lenticular, symmetrical wavy and hummocky cross-stratification-like, deformed (in macroscale)	From a few centimetres to 20 centimetres/sharp bottoms and tops/tabular with large lateral continuation, lenticular	Silica supply, production (diatom blooms), dissolution and precipitation (evaporation and salinity changes), primary and secondary diagenetic processes	Shallow-water (lacustrine or shelf), freshwater or brackish, associated with oscillatory flow	FAI, II
F3. Stratified marls	**Marlstone, silicified marlstone**	Very fine-grained, pelithic/ massive, bedded/light brown to dark brown/fish remains on separation surfaces	None/rarely subtle cyclic horizontal lamination, irregular or micro-lenticular (lamination most commonly indicated by colour change)	From 0.2 cm to several, even 20 cm /sharp bottoms and tops with facies F.1 and F.2/ gradational or sharp boundaries with cherts/tabular with large lateral continuation, wavy, lenticular	Supply, production of coccolith mud (algal blooms), dissolution and precipitation (evaporation and salinity changes), primary and secondary diagenetic processes; hemipelagic suspension	Shallow-water (freshwater to brackish), seasonally freshwater or brackish (freshwater supply) and then hypersaline (evaporation process within a shallow basin) or deposition in freshwater to brackish of a shelf that suffered extensive freshwater river output alternating with marine transgressions	FAI, II, III
F4. Sandy–pebby marls	**Marlstone, sandy–pebble marlstone**	Various grain size (matrix supported marlstone)/ compacted, massive or thick bedded/grey-brown to dark-brown/lithoclasts, fragments and whole shells of molluscsk	Lens shape, large scale cross stratifications (HCS), dome amplitude approx. 20–30 cm, wavelength 90–100 cm	Lack of bedding or lamination, if present as internal lamination of large scale HCS-like structures with weak or invisible bedding	Tsunami-induced deposition from highly concentrated suspension, induced by tectonic processes, deposition from wave-induced oscillatory flows	Shallow-water, freshwater or brackish dominated by carbonate sedimentation, reached by tsunamis (lacustrine, or inner shelf or shallow-ramp-type basin)	FAI, II
F5. Marly–mudstone heterolithics	**Marlstone, organic rich mudstone**	Very fine grained, pelithic (marlstones, mudstone), fine to medium grained (sandstone)/ laminated in millimetre scale, thin bedded, heterogeneous/ light brown to brown	Horizontal, wavy lamination in marl, lenticular and flaser in mudstone	From about 1 mm to 5 cm, total thickness about 1.5 m/sharp bottoms and tops/wavy, tabular	Alternating traction tidal currents and suspension during slack-water periods	Intertidal flat (Type 1), upper tidal flat (Type 2), with periodically changing basin morphology (open-closed basin), with varying amounts of *in situ* biogenic material supplied and produced, alternatively subtidal settings on the shelf	FAIII
F6. Stratified and laminated sandstone	**Very fine to medium grained sandstone**	Very fine to medium grained/ thin to medium bedded/grey, grey-brown-greenish	Ripple cross-lamination, lenticular flaser, horizontal lamination/ laminations are arranged in sequences	From about 1 mm to 10 cm/ sharp bottoms and tops, gradational between sedimentary structures/ stratified, tabular	Traction tidal currents deposition, cyclicity result of spring and neap tides	Tidal flat or tidal influenced shallow-water (fresh to brackish) inner shelf	FAIII

Fig. 3. Exposure of Dynów marls in the Sękówka riverbed (left bank) in Gorlice (section A). State of preservation of the exposure in 2015. Arrows indicate the bottom (on the right) and the top (on the left) of the studied section.

Facies F3: Stratified marls

Facies F3 (Table 1) is very well stratified with individual beds 0.2 cm to several tens of cm. thick (Fig. 10). The beds also have alternating different proportions of marl to marly mudstone, (from submillimetres to several centimetres). The colour of the marl is brown to dark brown. The marls are highly calcareous, in places slightly silicified (Fig. 10), or contain very thin layers or lenses of chert.

The marls of this facies do not exhibit any obvious internal sedimentary structures, and these may have been erased by diagenetic processes. However, subtle, irregular, cyclic horizontal laminations suggested by colour changes and laminations with a ?lenticular appearance are occasionally present. The marls show irregular, nested or layered silicification, and sometimes the marls are strongly silicified. For this reason they are often called cherts or siliceous marls (Świdziński 1947; Birecki 1964). Fish fragments are often found in the beds (e.g. section B). Some thin laminae or beds are limestone. This facies occurs in all three sections examined. Its thickness varies from tens of centimetres to several metres. It occurs together with facies F1, F2, and F4 (mainly in sections B and C). Petrographic studies of this facies show that the marls are composed of very fine-grained micrite, with dispersed clay minerals and detrital grains, mainly quartz, glauconite, pyrite and metamorphic rock (diameter 0.05–0.25 mm), as well as fine plant and organodetrital detritus and limonite which emphasise lamination. No bioturbation is observed. Contacts between marls and cherts are not sharp, but there are gradual transitions between them, and silica infiltrates irregularly into the mudstone/marlstone (Dziadzio et al. 2025).

Facies F4: Sandy–pebbly marlstone

Facies F4 (Table 1) occurs in sections, B and C (Figs. 5, 6, and 7), and is characterised by amalgamated beds or is thick-bedded. Where there is a clear bedded stratification, there are flat or lenticular beds on a large scale (Fig. 11). Internally, there are scattered grains with well-rounded quartz or other lithic components, in grain sizes up to 0.5 cm. There are also fragmented and well-preserved molluscs (cf. Studencka et al. 2016) varying in size from a few millimetres to 1 cm, with sporadic thick-shelled bivalves up to several centimetres in size. Marls of this facies can therefore be referred to fine-grained conglomerates. The colour varies from grey-brown to dark brown, and yellow-brown. Facies F4, usually has a sharp bottom and top and is about 1.3–1.5 m thick (Figs. 5 and 7). In section C, extensive inclined strata and lenticular strata are visible, strongly suggesting hummocky stratification (HCS) composed mainly of very fine-grained marl. The amplitude of the HCS domes is about 20–30 cm and the wavelength varies between 90 and 100 cm (Fig. 11). In some places there is a faintly visible horizontal bedding.

Petrography of those deposits are similar in both sections B and C. Within this facies, there are also poorly visible soft deformation structures which, in places, are silicified. They are sandy mudstones with a micritic carbonate matrix. They contain poorly rounded detrital grains of quartz, feldspar, metamorphic rock and detrital glauconite, as well as heavily damaged organodetrital fragments. There is also fine plant detritus, limonite, and fine grains of pyrite and hematite (Dziadzio et al. 2025). Also, no bioturbation is observed.

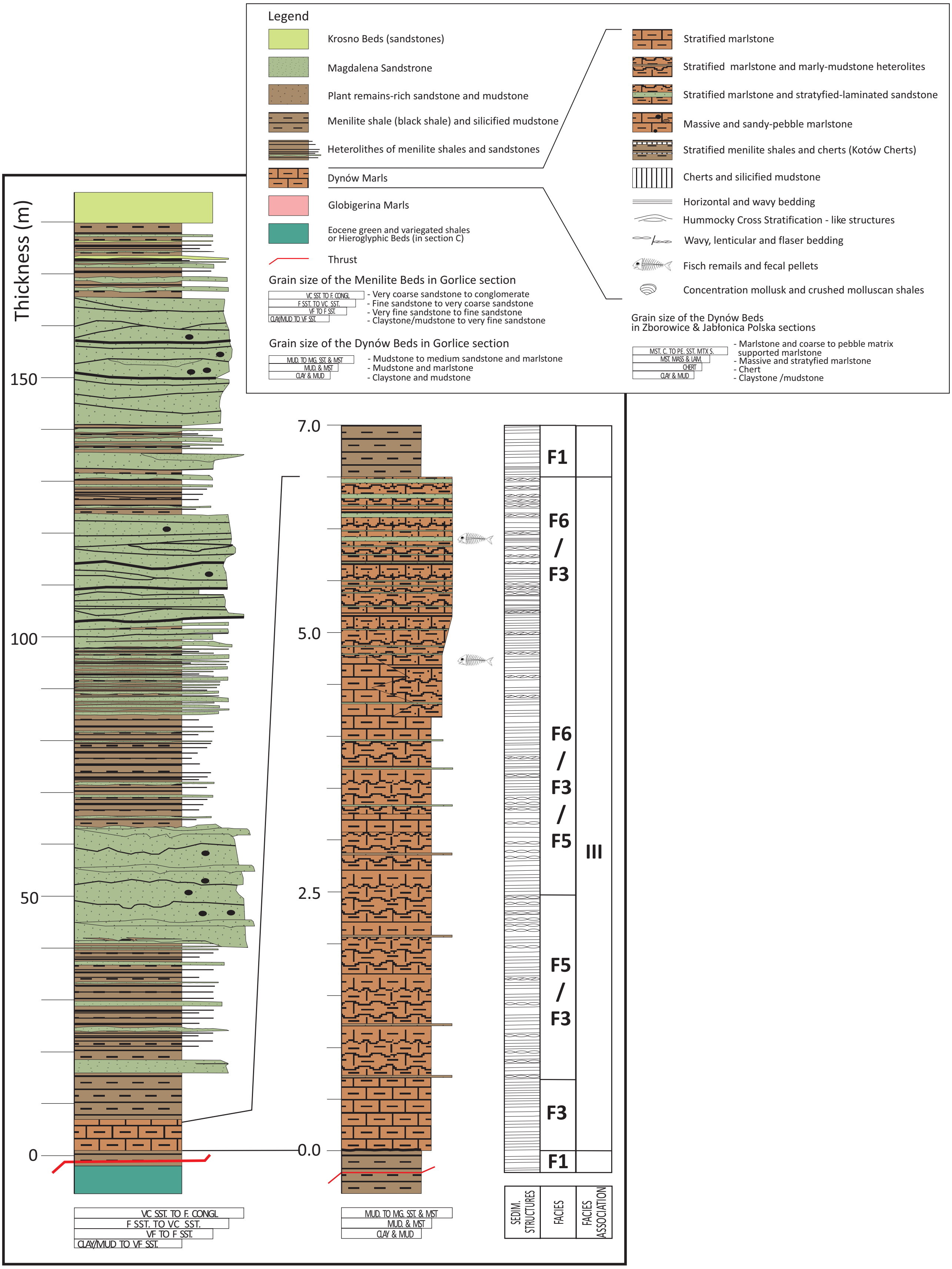

Fig. 4. Section A of the Menilite Beds and Dynów Marls (6,5 m thick) with the interpretation of facies and facies associations, partly based on the work of Dziadzio et al. (2016). Location: the southern limb of the Gorlice fold in Gorlice.

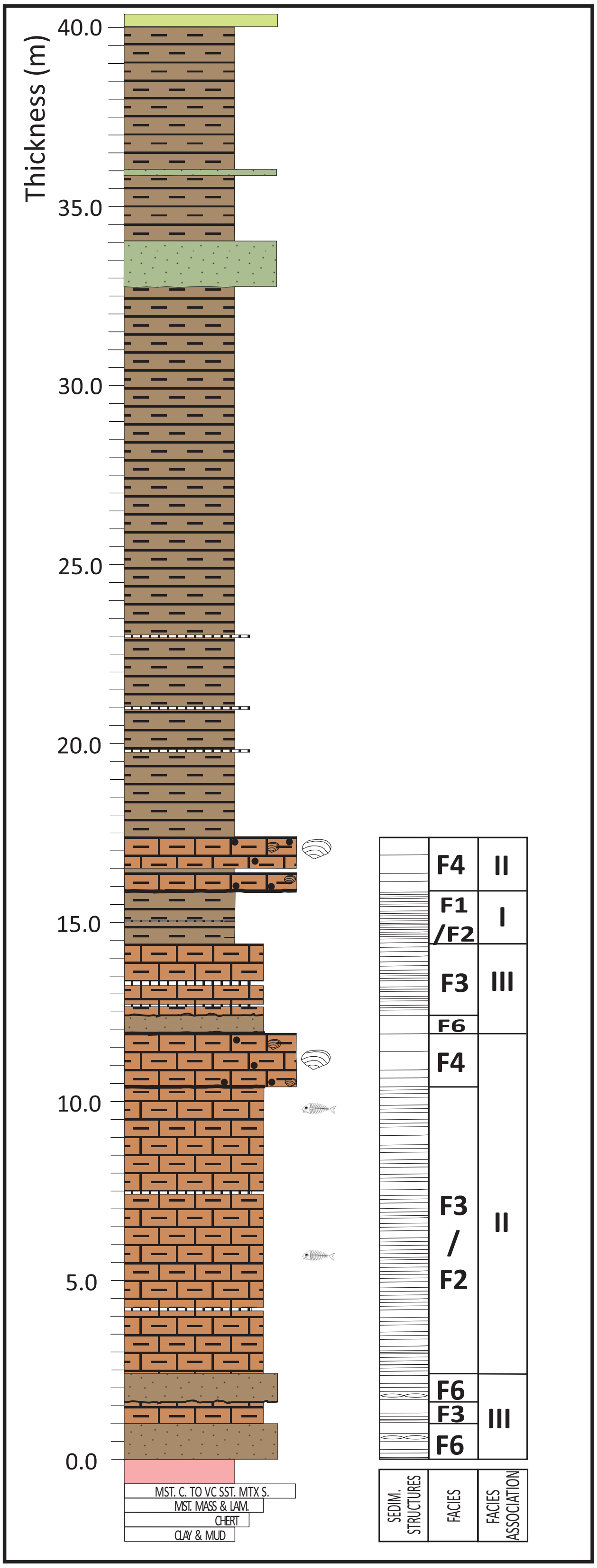

Fig. 5. Section B of the Menilite Beds and Dynów Marls with the interpretation of facies and facies associations on the southern limb of the Ciężkowice–Biecz–Osobnica–Bóbrka fold in Zborowice. For the legend see Fig. 4.

Facies F5: Marly-mudstone heterolithics

Facies F5 (Table 1) occurs only in section A. It is about 1.5 m thick and alternates with facies F3 (Fig. 4). It consists of two components:

(1) horizontally and wavily fine-laminated marl packages, without mudstones, from a few to tens of centimetres thick (Fig. 12) and

(2) mudstones and very fine-grained sandstones rich in organic matter (from 1 millimetre to several centimetres), with lenticular, flaser and wavy lamination (Fig. 13).

Type 1 is less common within facies F5 and is usually interbedded with thin, organic-rich, continuous laminations of unstructured mudstones ranging in thickness from a few millimetres to a centimetre.

Type 2 is characterised by alternating thin and very thin laminae and marl beds (also internally laminated) and calcareous, organic-rich mudstones/sandstones which, in addition to thin laminae and highly continuous beds, form lenses, often symmetrical, and beds with flaser lamination. The thin laminae and lenses of the mudstones are not lithified and break up into small scales or sand, while the surrounding marls are hard (partly silicified). The proportions of marls, mudstones and sandstones are variable and the facies is marl-dominated heterolithics. The marly parts, which weather white and light grey, more resistant to weathering, are carbonate and slightly silicified in places. Their colour on the fresh surface is brown. The light brown weathering parts are more mudstone and sandstone, poorly compacted, crumbling in scales (similar to Menilite shales), not carbonate. They are more susceptible to weathering, are not compacted and retain a similar colour on both the fresh and weathered surfaces. Mudstones and very fine-grained sandstones form symmetrical-ripple lenses and are covered by a thin marl lamina or a thicker interval of laminated marl. Marl laminae also occur within mudstone lenses as flaser lamination (Fig. 13). The marls are arranged in thin horizontal or wavy symmetrical layers with a wavelength of 10–20 cm (most commonly 10 cm). Within the mudstones/sandstones there are also small symmetrical ripples of low amplitude Facies F5 is interbedded with facies F3.

Facies F6: Stratified and laminated sandstone

The sandstones that make up this facies (Table 1) range in thickness from 1 mm to 10 cm. The sandstones contain horizontal, wavy, flaser and lenticular laminations (in places deformed horizontal or ripple laminations) as well as climbing, symmetrical ripple laminations and bimodal cross laminations and some laminae interfingering with mud deposits. In both types, no bioturbation is observed. Both types of deposit are interbedded with facies F3.

Sandstones interstratify with mud as heterolithics (Figs. 14–18). No bioturbation within this facies is observed. Mudstone and mudstone–sandstone intervals are rich in micas, organic matter, both plant and fish remains, and faecal pellets (fish coprolites) (Figs. 19 and 20). Their presence can be seen on

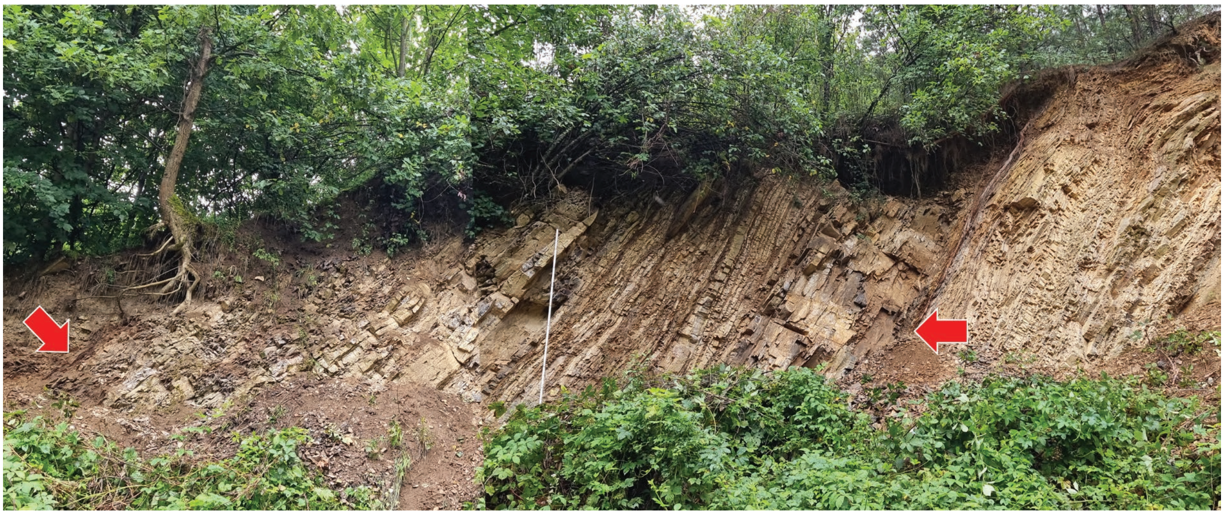

Fig. 6. Exposure of the Dynów Marls in Jabłonica Polska (section C). The state of preservation of the exposure in 2024. The arrow on the right indicates the bottom of the marl bed. The arrow on the left side of the photo indicates a tectonic zone that changes the angle of inclination of the beds and runs in the upper part of the Dynów Marls. A vertical scale (2 metres) is shown in the centre of the photo.

the surfaces of separation and in the perpendicular section. The sandstones are interbedded with thin marls, 0.2 to 2 cm thick, with sharp tops and bottoms, and some gradations of laminated sandstones/mudstones, which are well defined within the sandstones, but only after cutting.

In addition, within the finely laminated sandstones and mudstones, and less frequently marls, there are quite characteristic lighter and darker laminae, some of which can be interpreted as double mud drapes. Within the crossbedding there are mud drapes and reactivation surfaces (Fig. 17). They are composed of the same material, differing only in the degree of organic matter in the lamina. There are also alternating sandstone laminae and silt/clay laminae (Figs. 14, 15, 16, 17, 18, 19 and 20) and ripple marks with bimodal laminae (Fig. 18) and some laminae interfingering with mud deposits. This type of deposit is also found in the upper part of the Menilite Beds profile (Magdalena Sandstone), similar to the bimodal cross-lamination and interfingering of lamina sets with the surrounding mudstone sediments (Dziadzio 2018).

Sandstone–mudstone interbedding forms quite characteristic successions of sedimentary structures Fig. 21. The most common are from bottom to top: (1) mudstones or very fine-grained sandstones with lenticular and flaser lamination; (2) sandstones or mudstones, wavy laminated, horizontally laminated and again wavy laminated, lenticular and flaser laminated (Figs. 14 and 21); (3) horizontally and wavy laminated mudstones or very fine-grained sandstones; cross laminated, lenticular and flaser laminated sandstones, and successively wavy and horizontally laminated mudstones or very fine-grained sandstones (Figs. 15 and 21); (4.1) cross laminated, lenticular and flaser laminated (Figs. 17 and 21); (4.2) horizontally laminated mudstones or sandstones (Figs. 20 and 21). All these facies successions are bounded below and above by massive or very finely laminated marls of varying thickness. They also often pass into the next succession like the one below (Fig. 14). The facies successions are clearly cyclic (Figs. 14 and 22). Facies F6 is interbedded with facies F3, which varies in thickness from 0.5 to 10 cm (Figs. 4 and 22), and in the lower part of the section also with facies F5. Together they form an interval of about 4 m thickness in the middle and upper part of the Dynów Marl in section A (Fig. 4). Towards the top of the section, the proportion of sandstones and their thickness gradually increase.

In addition to laminated sandstones, this facies includes massive, structureless, multi-grained sandstones of brown or grey-brown colour, sometimes horizontally bedded and sometimes finely and subtly striated (weakly visible ripple lamination) with dispersed glauconite grains and large amounts of dispersed organic matter. They occur mainly in section B, in its lowest part. Their thickness is about 1 m. They were also previously described by Birecki (1964).

Facies association

Facies association FAI: Facies F1 and F2

This association is often found within the Menilite Beds. It is most abundant in the lower part of the Dynów Marls (although not exclusively, cf. Section B, Fig. 5). It is important because of its wider context and position, as well as the occurrence of this association within the Dynów Marls. A characteristic feature of this association is the heterolithic character or cyclic repetition of facies within it.

Facies association FAII: Facies F3 and F4 (with subordinate F1 and F2)

This association, typical of the Dynów Marls (Figs. 5 and 7), contains mainly horizontally bedded marls (F3), often separated by submillimetre-thick claystones or mudstones of F1,

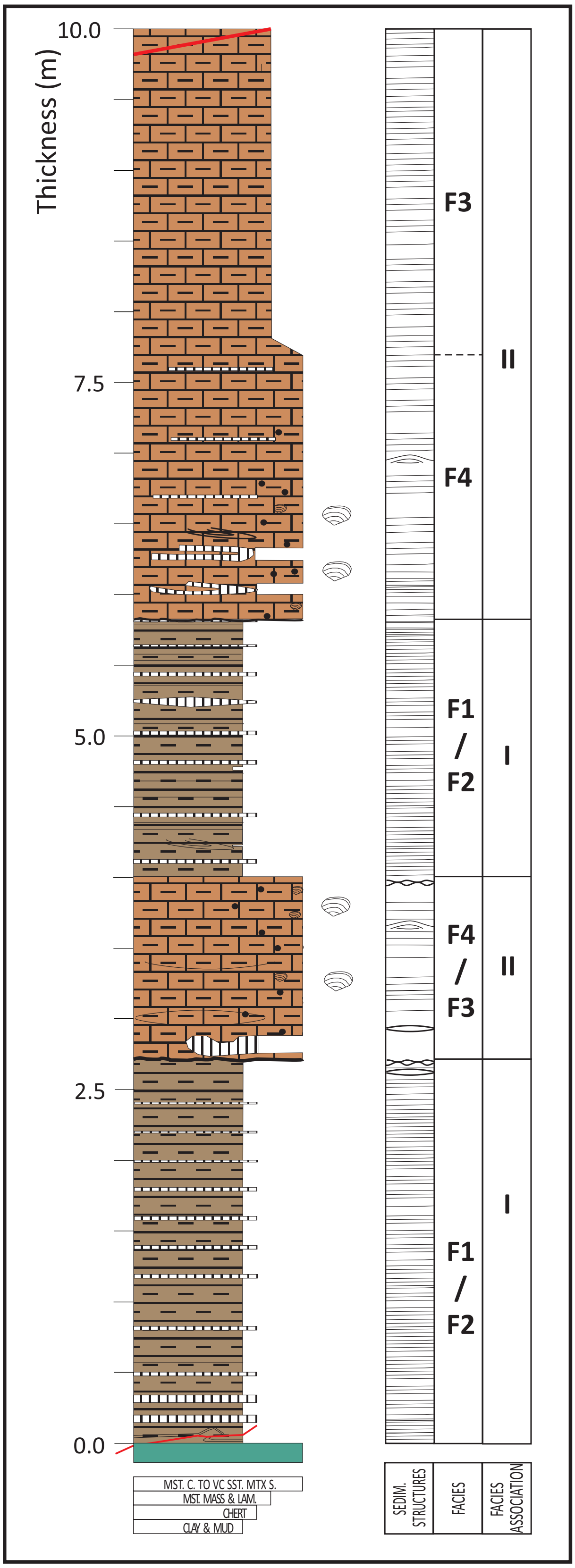

Fig. 7. Section C of the Menilite Beds and Dynów Marls with the interpretation of facies and facies associations on the southern limb of the Turze Pole–Zmiennica fold in Jabłonica Polska. For the legend see Fig. 4.

Fig. 8. Facies F1. The lower part of the Dynów Marls (siliceous marls). Visible facies contrast of weathered white marls – upper part of the photo, and brown Menilite shales (mudstones) – middle part of the photo, and more argillaceous – lower part of the photo (above the hammerhead). Within the shales a symmetrical wavy bedding is visible. Section A, location: Figs. 1, 2 and 3; scale: hammerhead 18 cm.

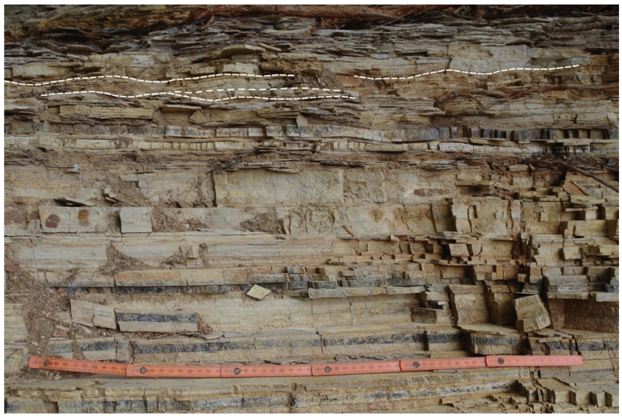

Fig. 9. Facies F2. Parallel stratified cherts. The upper part of the photo shows a gradual transition to Menilite shales (facies F1). Symmetrical wave and lenticular sedimentary structures are present in the shales. The actual dip angle of the beds is about 85° (photo is rotated). Outcrop in Jabłonica Polska (Kotów Cherts). Section C, locality: Figs. 1B and 6; scale at bottom of photo: 1 m.

Fig. 10. Facies F3 Stratified marlstone. Subtle horizontal lamination visible within thinly bedded brown marls. Outcrop in Jabłonica Polska. Section C, location: Figs. 1 and 6. Hammerhead (18 cm) for scale.

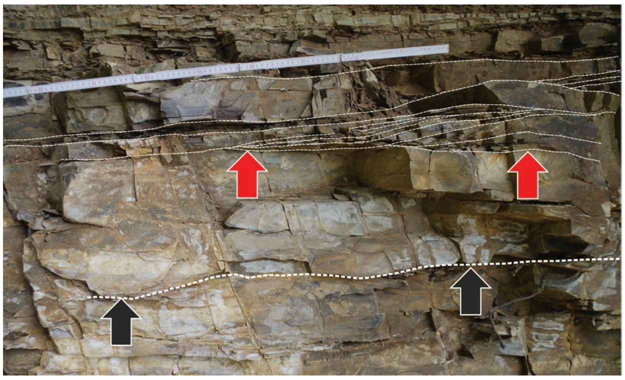

Fig. 11. Facies F4. Massive and sandy-pebble marlstone. In the lower part, an irregular erosional–depositional surface (black arrows). In the upper part a large lenticular bed (HCS) is visible (red arrows). The actual dip angle of the beds is about 85° (photo is rotated). Section C, location: Fig. 1, photo 2, scale 50 cm.

Fig. 12. Facies F5. Heteroliths of finely laminated marls and horizontally and wavily laminated mudstones with a gradual upward increase of mudstones. Lower part of the Dynów Marls in section A. Location: Fig. 2. Hammerhead (18 cm) for scale.

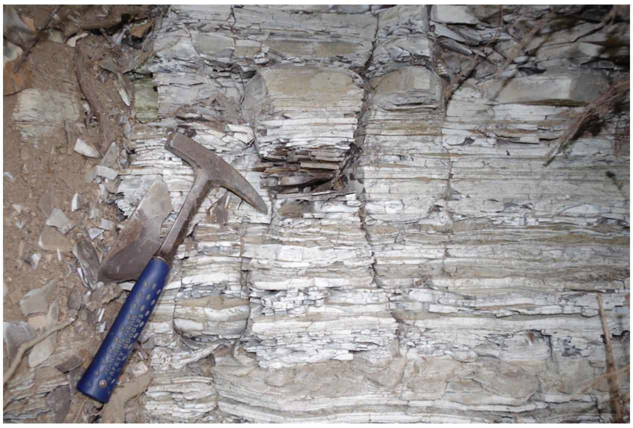

Fig. 13. Facies F5. Heteroliths of marls and laminated mudstones. Lighter beds are marls, darker beds are organic mudstones and very fine-grained sandstones of the Menilite shale type. In the lower part of the photo, the mudstones show a slightly wavy horizontal lamination with a wavelength of about 20 cm. In the middle and upper part of the photo, there are marls with lenticular and flaser lamination within mudstones and sandstones. Location: Fig. 1. Hammerhead (18 cm) for scale.

and cherts (F2), which are subordinate thin beds and lenses within the association. In places the marls are silicified. In silicified marls there are irregularly distributed, often diffuse, concentrations of silica. Apart from subtle horizontal laminations, the marls themselves show no distinctive features. This association contains also structureless, sandy conglomeratic marls with shallow-water fauna and shell fragments (facies F4), as well as soft-sediment deformed beds. More importantly, however, FAll contains hummocky? and swaley strata (Fig. 7).

Facies association FAIII: Facies F3, F5 and F6

The facies succession in the third association, which occurs only in section A, should be considered in continuity and vertical succession (Fig. 4), because within it there are changes related to different proportions and types of facies, as well as changes in grain size and thickness upwards. The association consists of three facies, which gradually replace each other towards the top of the Dynów Marls section. In the lowest part of the association there are slightly silicified and well-bedded marls (F3). Higher up in the section there are bedded laminated marls of heterolithic type (F5), which pass into cyclically interbedded marls of facies F3 and sandstones of facies F6. In the upper part of section A (Fig. 4), the proportion of sandstones and mudstones gradually increases.

Discussion

It should be noted that the various facies and facies associations (within the same age interval) record changes in lithology and sedimentary structures. However, only some of these features are environmentally diagnostic and can be reliably used to interpret depositional environments. Despite this, the analysed sedimentary record does not present significant interpretive uncertainties. Other analytical methods, such as biomarker studies, have proven effective in identifying the genesis of non-diagnostic facies and in reconstructing depositional settings. This approach strongly supports environmental interpretations, showing excellent correlation with sedimentological data (Dziadzio et al. 2025).

Facies and facies association interpretation

Facies association FAI: Facies F1 and F2

Facies Association FAI comprises Facies F1 and F2 (see Table 1 and Figs. 5 and 7). These facies coexist and are genetically related.

Facies F1 formed mainly through the deposition of fine-grained material from hypopycnal suspension. Some of the organic-rich mud layers may also have originated from river-generated, hyperpycnal underflows that become muddy on the mid to outer shelf (Zavala et al. 2021).

Fig. 14. Three successive sandstone beds of facies F5 separated by thin marls layers. There is a similar sequence of sedimentary structures in the lower and upper beds (Sq. 1). These are flaser and lenticular laminations formed during the period of the more energetic spring tides and, in their central part, horizontal and slightly wavy laminations formed during the period of the less energetic neap tides. Such cycles are often bounded at the top and bottom by a bed or lamina of marl, or merge into the next sequence (upper sequence, and upper right part of the photo). The thin middle cycle is bounded by very thin marl laminae with lenticular lamination in the sandier parts and represents 4.1 type sequence (Sq. 4.1). Upper part of the section A. Location: Fig. 1.

Fig. 15. Facies F6. Wavy, flaser and lenticular laminated and locally deformed glauconitic sandstones. Horizontally laminated marls in the lower and upper parts of the picture. The cycle has the nature of sequence 3 (Fig. 21). The lower and upper parts may correspond to sediments deposited during neap tides, and the middle part to the period of more energetic spring tides. Such a vertical sequence may represent a record of a cycle deposited during a synodic month, Fig. 5, (cf. Tessier 1993; Kvale et al. 1995; Tessier et al. 1995). The upper part of section A. Location: Fig. 1. Scale: lens cup 5 cm.

Fig. 16. Facies F6. The lower and upper parts show horizontal and slightly wavy laminae formed during the period of less energetic neap tides. Each of the thin laminae may represent a single tidal episode. In the central part of the image there is flaser lamination formed during the period of more energetic spring tides (case (3), Fig. 5). It is probably a record of a single cycle deposited during a synodic month. Upper part of section A. Location: Fig. 1.

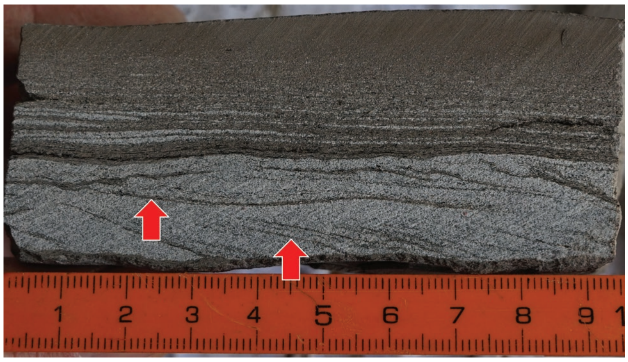

Fig. 17. Facies F6. In the lower part of the picture is a flaser lamination, in the upper part is a symmetrical lamination. The lower arrow indicates double laminae characteristic of tidal phenomena. The upper arrow indicates the reactivation surface. In the central part of the image are horizontally laminated mudstone and sandstone, passing into structureless and normally graded marl (case of sequence 4.1, Fig. 5). Central part of section A. Location: Fig. 1.

Fig. 18. Rhythmite-type deposits represent sequence (2), Fig. 21. Bimodal (herring bone type) lamination in the lower and upper parts and some laminae interfingering with mud deposits.

The frequent occurrence of subtle, thin laminae within Facies F1 may be due river-flood across the shelf and to accumulation that was interrupted by the transport of silt or larger grains along the bottom (Lazar et al. 2012, 2015). Unrug (1980) suggested the presence of sand and silt laminae within the Menilite Beds of Skole Unit as contourites resulting from deep-sea traction currents travelling along the deepwater slopes. These laminae are sometimes cross-bedded or ripple-laminated and occur in the form of lenses, as seen in facies F1 (Fig. 8).

Facies F1 also commonly exhibits low-amplitude, wavy, symmetrical and lenticular beds of various wavelengths. These structures, resemble hummocky cross-stratification, which is most commonly associated with storm processes and may have formed through complex or oscillatory flows (e.g., Dott

& Bourgeois 1982; Arnott & Southard 1990; Yang et al. 2006; Cummings et al. 2009; Tinterri 2011). Hummocky cross strata is common along shoreface areas but also extends far out on the shelf (Dott & Bourgeois 1982). However, it cannot form below storm wave base, i.e., up to 30–50m of water depth on the shelf. It is described from many modern and ancient subaqueous deltas that transit across modern shelves (Patruno et al. 2015; Rossi & Steel 2016; Rossi et al. 2017).

They can also be associated with the development of intrabasinal gravity waves, occurring at different depths depending on the position of the pycnocline (including its seasonality) within the sedimentary basin (Morsilli & Pomar 2012), but this is difficult to prove.

The interpretation of this facies is supported by the results of biomarker studies, which provide reliable indicators of the depositional environment. According to the obtained data, the depositional environment was anoxic, freshwater or brackish, and of a lake-type. The setting could possibly also represent inner to mid-shelf zones that are dominated by fresh-water river outflow, sometimes for some 10s of kms basinward from the marine shorelines (Zavala et al. 2021). The environment was episodically supplied with both terrestrial and marine organic matter (Dziadzio & Matyasik 2021; Dziadzio et al. 2025). Small gypsum crystals were also found within this facies (Dziadzio et al. 2016), further suggesting periodic evaporation possibly during times of low eustatic sea level. This type of deposit can also accumulate in areas that are periodically isolated, such as bays, estuaries, lagoons, and coastal lakes, where low-amplitude, symmetrical, wavy bedding is present (Tinterri 2011).

Finally, the collected data suggest that this facies was deposited in an isolated, shallow-water (lacustrine or freshwater inner shelf), partly brackish, periodically high-energy, evaporitic sedimentary basin (or within a coastal lake, bay or lagoon).

While the genesis of facies F1 is most likely as outlined above that of facies F2 is more difficult to interpret. Cherts (facies F2) have traditionally been interpreted as the result of marine deposition in a deep-water environment (Pisciotto & Garrison 1981; Pisera 1991; Iijima 1994). Their sedimentation is also associated with shallow-water carbonate environments or associated environments (e.g., Tucker 1991; Einsele 1992; Sugitani et al. 1998; Bustillo et al. 2002). However, chert deposits are commonly also formed by secondary diagenetic processes (e.g., Hesse 1989; Einsele 1992; Sugitani et al. 1998; Maisano et al. 2020, 2021). Bedded cherts can also be the result of compaction and recrystallisation of silica-rich biogenic sediments composed of unicellular organisms (radiolaria and diatoms or sponge needles) in both marine and lacustrine sedimentary environments.

In interpreting facies F2, it should be noted that the sedimentation of Menilite shales and cherts in the Oligocene is related to the period of isolation and freshening of the Paratethys. The climate at that time characterised by seasonality, with cool, wet winters and warm, dry summers (Mosbrugger & Utescher 2005; Mosbrugger et al. 2005). This may favour chert occurrence, according to recent interpretations, that some of the siliceous sediments were accumulated in specific shallow depositional environments (Gammon et al. 2000; Ehrenberg et al. 2001). Their formation is associated with sedimentation on a ramp-like shelf under cold water conditions (Gates et al. 2004). To determine whether such a process was possible in the case of facies F2, detailed paleoclimatic studies would be required.

In the study area there are no cherts in section A, but silicified marls of facies F3 are present (see interpretation of facies F3). In section B, facies F2 occurs (also with silicified marls), which may indicate a change in depositional conditions, or even a different zone (possibly slightly deeper or closed). In section C, symmetrical wavy and hummocky cross-stratification-like structures are preserved in the cherts, which likely indicate shelf-storm induced depositional conditions and influence of oscillatory flow (e.g., Tinterri 2011).

Undoubtedly, the main factor in this case was the supply of silica, most likely resulting from mass blooms of diatoms and the long-term deposition of diatomite associated with low salinity (due to the influx of fresh water), climatic cooling, and increased seasonality (Krhovský 1981). Other studies (Kotlarczyk 1966; Kotlarczyk et al. 1986; Kotlarczyk & Kaczmarska 1987; Kotlarczyk & Leśniak 1990; Pupp et al. 2018) also indicate their presence in the profiles of the Menilite Beds.

The coincidence of basin phenomena (shallow but morphologically very diverse sedimentary basin or basins), as well as climatic, biological (diatoms prefer colder climates – Wikipedia entry on diatom) and physicochemical (evaporation processes and salinity changes) conditions could, on the one hand, lead to the production of organic silica, of basin origin and its delivery to shallow environments, but also to its production in shallow, often freshwater or brackish zones (both stenohaline and euryhaline species occur in many diatomite horizons, Kotlarczyk & Kaczmarska 1987).

Diagenetic processes associated with evaporation could also have led to the dissolution and reprecipitation of silica (Einsele 1992; Sugitani et al. 1998). Under favourable conditions silica could have been dissolved and precipitated as chert, or it could have migrated and silicified the surrounding rocks, as observed in silicified marls. This phenomenon is evident also in cherts with sedimentary structures, such as the silica impregnation of primary sediments (see Dziadzio et al. 2025).

No biomarker studies were performed on the cherts. However, the interpretation was supported by the results of studies by Jirman et al. (2019, 2020). Regarding the chert deposits underlying the Dynów Marls in the Czech Republic, Jirman et al. (2019, 2020) suggest that they are associated with a mass bloom of diatoms (see also Schulz et al. 2004) that inhabit shallow brackish and freshwater environments (evidenced by the presence of red algae and the absence of significant terrestrial input). Facies F1 occurs alongside facies F2 (facies association FAI), this could suggest that both formed in similar shallow-water lacustrine or shelf conditions, with additional

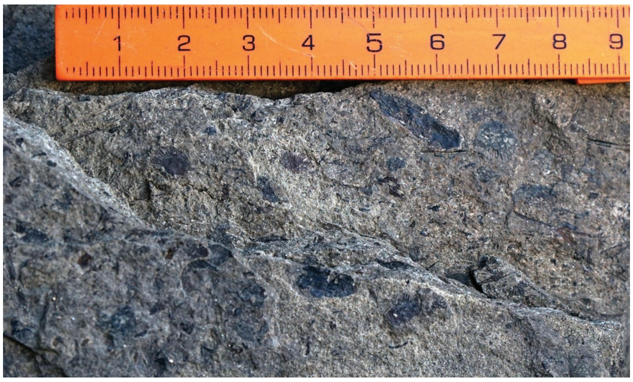

Fig. 19. Facies F6. Surface of separation from the sandstone-dominated interval. Visible large accumulation of fish remains, skeletal fragments, fins and scattered lighter submillimetre faecal pellets. Central part of section A. Location: Fig. 4.

Fig. 20. Facies F6. Subtly laminated marly sandstone. The lumpy structure in the lower part of the picture is caused by the presence of fish fragments (darker, flat streaks) and faecal pellets (lighter, lenticular and oval). In the upper part of the image there are sets of double mud laminae. Middle part of section A. Location: Fig. 4.

evidence of the ingress of freshwater and diatom blooms. Such conditions can also be present within a coastal lake, bay or lagoon, but there is no indications of subaerial exposure in the stratal succession.

Facies association FAII: Facies F3 and F4 (subordinate F1 and F2)

Facies Association FAII (see Table 1 and Figs. 5 and 7) comprises two, and occasionally three or four facies (F3 and F4, and locally F1 and F2) in alternations.

Rhythmic alternations of limestones and marls/mudstones (shales) are known from a variety of depositional environments, from coastal to distal shelf zones (e.g., Einsele et al. 1991; Pittet et al. 2000; Walker et al. 2002; Arzani 2006). They include well-stratified to nodular successions with relatively high carbonate content (limestone) and relatively low carbonate content (marl). Despite the importance of these formations, it is still not well understood how they are formed (Nohl et al. 2019). A similar situation occurs in the case of limestone/marl and mudstone and marl, as well as cycles with chert and requires an interdisciplinary approach, especially a look at modern shelves, to explain their genesis. Therefore, the whole sedimentary succession and the facies diversity occurring within it should be studied in order not to exclude various genetic factors (Hallam 1986).

A number of studies have been carried out to interpret the origin of rhythmic alternations of limestones/marlstones and marlstones/mudstones, including not only sedimentological, geochemical and isotopic studies (Bottjer et al. 1986; Eicher & Diner 1991), but also astrochronological studies (e.g., Berger et al. 1984; Bellanca et al. 1996), although these

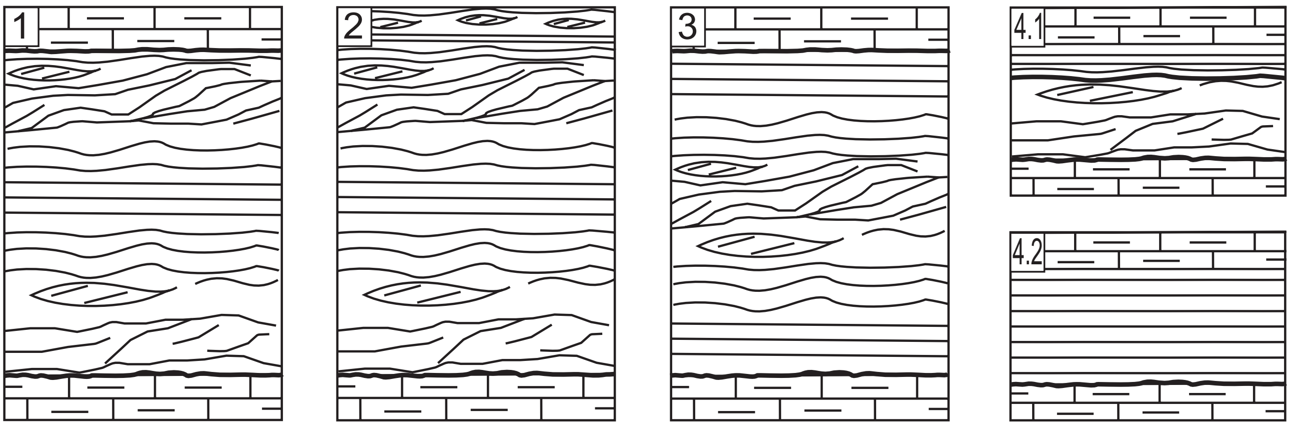

Fig. 21. Sequences within cycles, probably related to different periods of the synodic month (29.5 days). (1) A sequence within which, from the bottom, there are spring tide deposits (corresponding to the new moon), neap tides (corresponding to the first quarter), and again spring tide deposits (corresponding to the full moon), and then the last quarter. This sequence represents a complete synodic cycle. The sedimentation of the marl deposits probably also occurred during neap tides. (2) The first sequence type (1), does not end with a marl layer. Instead, it reappears as wavy, horizontal, lenticular and flaser lamination at the beginning of the next sequence. (3) A case in which the neap tide of the first quarter may not be noticeable. (4.1 and 4.2). Cases of incomplete synodic cycles (neap or spring tides) that are missing various sequence elements, most likely due to erosion.

have been inconclusive (Hallam 1986; Bathurst 1987; Westphal 2006; Li et al. 2018). These studies have also often assumed that depositional records are related to Milankovitch cycles, which must be treated with great caution (Hallam 1986; Arzani 2006).

There is also some debate about the origin and mineralogy of the dissolved carbonate phase, the timing and burial stages at which carbonate is redistributed, and the influence of primary sedimentary properties on the diagenetic redistribution of carbonate (e.g., Nohl et al. 2019; Westphal 2006; Westphal et al. 2008). Two models are proposed to explain their origin: (1) via redistribution of carbonates as a result of late diagenetic dissolution under pressure, or (2) via early diagenetic dissolution of aragonite and reprecipitation of calcite (differential diagenesis model).

Both models may imply different interpretations of paleoenvironmental conditions. Identification of the formation process is therefore essential. From many cases studied, it appears that most stratified limestones and marls are formed at the stage of early diagenesis (i.e. carbonate redistribution), i.e. aragonite dissolution and reprecipitation as calcite (Nohl et al. 2019).

In case of facies F3 (also with thin intercalations of facies F2) lack clear sedimentary indicators of their sedimentary environment.

Depositional processes consisted of the supply or production of large amounts of organic mud, and it should be noted that the discharge of most rivers reaching the coastline consists of at least 80 % terrestrially derived mud, often organic rich. Coccolith mud (the main component of the Dynów Marls, see Haczewski 1989) and diatom mud are also a source of silica.

Their presence is the result of the mass bloom of algae (Pupp et al. 2018) and their deposition and diagenesis, at a low sedimentation rate (for the sedimentation of Menilite Beds, the rate is considered to be relatively low, 25–35 m/Myr, Malata & Poprawa 2006) may favour suggest the differential diagenesis model.

It is likely that the dissolution of siliceous skeletal elements and their precipitation under hypersaline conditions, such as may exist in lagoons, coastal lakes – periodically cut off from water supply or periodically supplied with water – may be the cause of the dissolution of opal skeletal elements and subsequent precipitation of silica within the still poorly diagenetic marly sediment (Einsele et al. 1991; Einsele 1992; Sugitani et al. 1998). The occurrence of irregular, scattered silica impregnations and silica horizons interbedded with marls, as well as their relationships, likely indicate a post-depositional genesis (Dziadzio et al. 2025), for example late diagenetic dissolution under pressure – the first type of origin.

Fig. 22. Interbedded marls of facies F3 and sandstones of facies F6, forming characteristic cycles that repeat one after the other. These cycles are probably related to tidal processes. S – Deposit formed as a result of spring tides (or synodic cycles), N – Deposit formed as a result of neap tides (end of synodic cycles, or formed as a result of isolation of the basin from the influence of tidal processes and deposition from suspension). Location: Fig. 4.

The presence of characteristic biomarkers of saturated and aromatic fractions indicates both freshwater and saline condition and some of them indicate evaporation.

The presence of algal substances also suggests that this facies was deposited in a closed or periodically closed basin with fluctuating salinity, most likely due to variations in the supply and evaporation of freshwater (Dziadzio et al. 2025). Floodwater influx alternating with even small rises of sea level will cause such salinity alternations on the shelf, with evaporation on the innermost shelf during lowstands of sea level. In Icehouse periods such as during some of Oligocene, 40–60m sea level changes occurred with high frequency (80–150Ky) (Miller et al. 2020; Haq & Ogg 2024).

Facies F3, based on the facies context and current knowledge, may have been deposited in a shallow-water (freshwater to brackish) lake-type basin with periodic hypersaline conditions. An alternative explanation would be on the freshwater to brackish reaches (seaward of the shoreline) of a shelf that suffered extensive freshwater river output alternating with marine transgressions. Many modern shelves are like this as evidenced by the repeated, very low-angle (0.5 degree) advancement of upward-coarsening clinothems (20–50m high) creating muddy subaqueous delta lobes, in alternation with intervals of open marine flooding (Denommee et al. 2016).

From an interpretative point of view, facies F4 has a rather complex set of sedimentary characteristics. These include a massive nature; sharp bottom-to-top and intra-bed boundaries; a lack of bedding or lamination; and the presence of large-scale HCS-like structures. The facies contains a scattered lithic component of various sizes and shallow-water bivalve fauna including large individuals with rounded shell edges. The general nature of this facies is similar to storm- or tsunami-type deposits that are common on open marine, wave-dominated shelves and form in water depths down to storm wave base (commonly 40 m).

Many examples and interpretations of such deposits have been described in the literature, mainly from clastic successions, (e.g., Dam & Surlyk 1993; Myrow & Southard 1996; Bondevik et al. 1997; Dawson & Smith 2000; Fujiwara et al. 2000; Myrow 2005; Bourrouilh-Le et al. 2007; Morales et al. 2011; Morales 2022).

When this layer is found on the coast, it can easily be confused with storm layers, although in confined environments and sheltered bays, such as lagoons, deltas, estuaries or mudflats, it is easily recognisable as different from the muddy sediments normally deposited in these environments, and storm sediments do not extend as far landwards (Morales 2022). However, storm beds are often deposited on top of the muddy embayment strata during minor transgressions (Cattaneo & Steel 2003). In this setting they are characterised by a fining-upward facies succession (caused by upward deepening of the water) with sharp-based shell lag deposits and shells and shell fragments irregularly distributed in a sandy–muddy matrix and granular sediment with an erosional base, often ending with a bioturbated layer. An important feature of such a transgressive unit is the large number of molluscs, including open sea species mixed with others typical of wave-protected environments (typical of inland systems, including euryhaline bivalves). These deposits are also rich in microfaunal assemblages, especially diatoms and ostracods. Sometimes such beds are cross-laminated. There are also examples of structureless tsunamite beds consisting of a clay-mud matrix and various rock fragments of different sizes and types, often containing fragments of marine organisms from isolated areas (Morales et al. 2011; Morales 2022). Tsunamites can also form complex lithotypes that are repeated in the profile and show no bedding or only very subtle lamination (Bondevik et al. 1997).

They all have erosional bases (wave ravinement surfaces) and extend for tens of kilometres along the coastline in environments previously characterised by wave energy, low slope, muddy shores and abundant fine-grained sediments, such as those found on deltaic plains or mudflats. In all cases, these sediments show a characteristic accumulation of heavy metals (Pb, Cu, Ni, Fe and/or Cr) (Whelan & Kelletat 2005).

Sometimes such beds are cross-laminated and contain well-developed HCS-type bedding and other structures associated with wave-storm processes as result of combined flow in the zone above the storm wave base (Dott & Bourgeois 1982; Duke et al. 1991; Dam & Surlyk 1993), (cf. facies interpretation F1) and also from tidal flat environments (Yang et al. 2006; Tinterri 2011). In this zone, the wavelength of these structures can be smaller than in the outer shelf zone. This is due to the presence of a wide, shallow subaqueous platform where wave development is limited (i.e. wave height is limited by depth). The maximum size of the HCS may increase with decreasing water depth from the shelf break to the inner shelf and then may decrease landward from this point because wave size is limited by depth (Yang et al. 2006).

In facies F4 almost all of these features are present. The HCS-like structures found in section C have the characteristics of structures formed by sediment-laden and wave-induced oscillatory flows and can be deposited in a coastal, shoreline environment (see Tinterri 2011). During transgressions they can also occur in an environment previously dominated by river-dominated hyperpycnal flows in the lower coastal zone (e.g., Jelby et al. 2020), but the facies context suggests a relatively shallow zone.

Biomarkers from this facies originate from various depositional environments but consistently indicate anoxic, brackish-to-freshwater conditions as would be expected in coastal and inner-shelf zones. Some also suggest a cold climate (Dziadzio et al. 2025).

The massive and sandy–pebble marlstone of this facies could have formed as a result of transgression during tsunami-related processes induced by deeper-water thrust-tectonic activity in the Lower Oligocene (Dziadzio et al. 2016, 2019). Another important fact is that this facies occurs and is petrographically similar in sections B and C (e.g., the same type of the deposits and presence of detrital glauconite grains, Dziadzio et al. 2025), which are about 70 km apart, with the original distance between the depositional zones reaching up to 100 km. Most probably, the two tsunamite levels occuring in both sections are the same, Figs. 4, 6 and 23).

The context of the facies suggests deposition in a shallow-water (lacustrine or inner shelf) environment, most likely a shallow-ramp-type basin where the seaward-dipping clinothems have very low angles (up to 0.5 degree; Patruno et al. 2015). This environment could well have been periodically isolated from the influence of the ocean, though not during time periods showing tidal rhythmites. This isolation could have preserved the deposits, which are interpreted to be the result of a tsunami (see, for example, Morales et al. 2011; Morales 2022). This interpretation is consistent with paleogeographic reconstructions, which indicate a reduced size and salinity of the Paratethys during this period, as well as with tectonic activity in the Lower Oligocene that could have

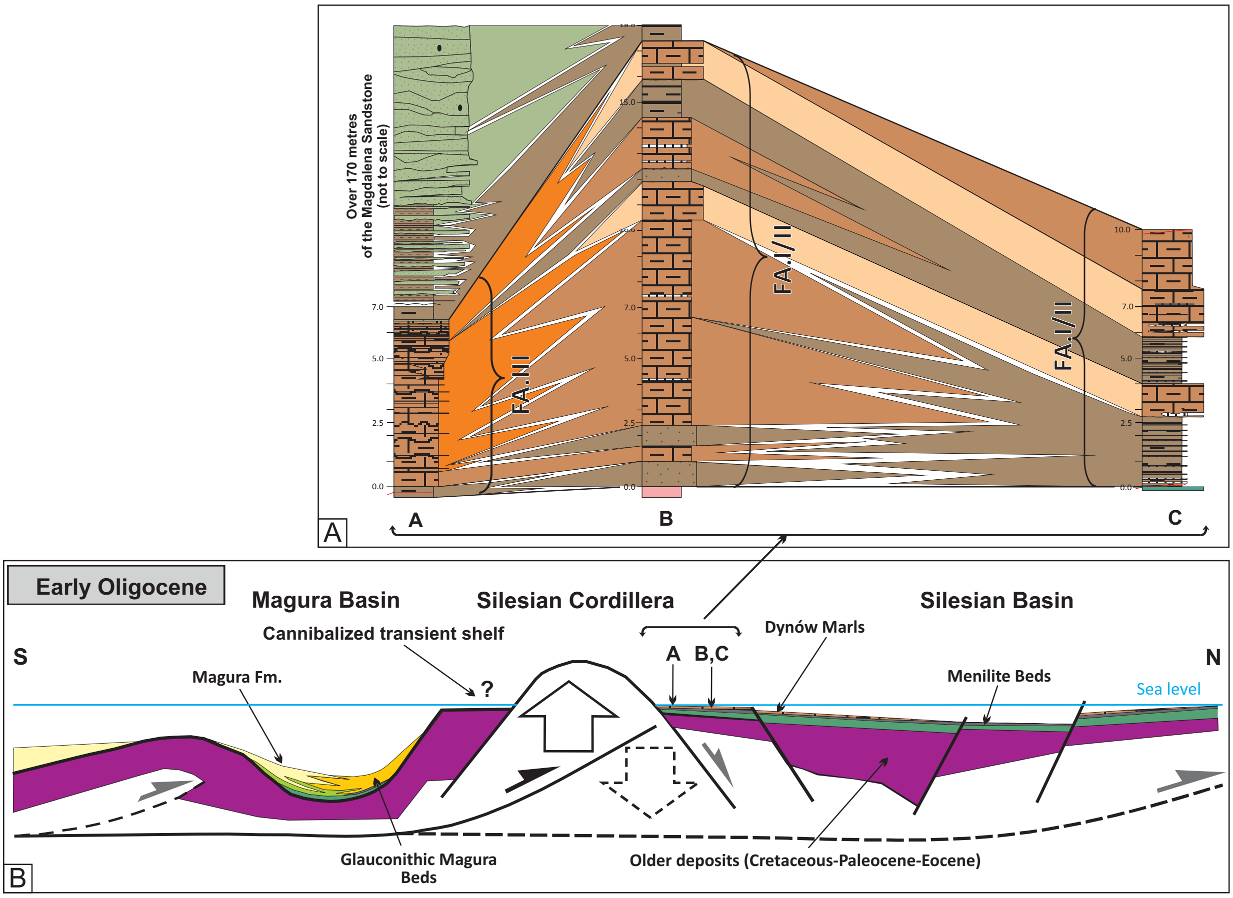

Fig. 23. A schematic, hypothetical model (not to scale) of early Oligocene sedimentation on the northern flanks of the emerging Silesian Cordillera (between the Magura and Silesian basins) for the Dynów Marls. **A** — Simplified facies association correlation between sections A, B and C. In section A, the Magdalena Sandstone, which is schematically drawn, developed on the Dynów Marls and represents a shallow-water deltaic complex (see Dziadzio 2015a, b for details). **B** — The model illustrates the positions of sections A, B and C, taking into account the genetic interpretation of facies and their associations. The shallow-water deposits of sections A, B and C are preserved by burial when the shelf eventually founders, separating the Silesian Basin from the Skole Basin by another blind thrust anticlinal cordillera (based on Dziadzio et al. 2016). This is especially visible in the area of section A.

triggered tsunamis and deposited diverse material in shallow environments.

This association may have been deposited in a large, shallow, lake-like basin, or in the coastal zone of a paleomorphologically diverse lake, or alternatively on a shelf that at times was dominated by freshwater river outflow and at other times by rising relative sea level and transgressive deposits such as the sandy HCS beds.

Facies association FAIII: Facies F3, F5 and F6

Facies Association FAIII (see Table 1 and Fig. 4) is present only in Section A and comprises three facies: F3, F5 and F6 facies (see Fig. 4). The facies F3 sharply overlies the Menilite shales (facies F1), reflecting a rapid change in basin conditions, likely due to the influx of river freshwater and nannoplankton blooms. Above the lower interval dominated by facies F3, the heterolithic deposits of facies F5 gradually transition to cyclically interbedded marls of facies F3 and F5. Facies F5 is characterised by two types of sediment: (1) horizontally and wavily fine-laminated marl packages, without mudstones, from a few to tens of centimetres thick (2) mudstones and very fine-grained sandstones rich in organic matter (from 1 millimetre to several centimetres), with lenticular, flaser and wavy lamination which provide support for the interpretation of the facies.

The environment in which these types of sedimentary structures were deposited can be deduced from well-documented modern sedimentary environments, such as the Bay of Mont-Saint-Michel in Normandy (Tessier 1993; Tessier et al. 1995); from the beaches of the barrier island of Schiermonnikoog (North Sea, Netherlands) (Kremer et al. 2008) and Paso Seco in Argentina (Maisano et al. 2020, 2021), as well as past environments, such as those described by Gerdes (2007), Kremer et al. (2008), Cuadrado (2020) and Maisano et al. (2020).

The Bay of Mont-Saint-Michel (Tessier 1993; Tessier et al. 1995) is one of the most representative examples of a macrotidal coastal environment. In this setting, laminated, very fine sandy or silty sediments are deposited during spring tides, and when tidal energy decreases (during neap tides), the settling of clay and silt from weaker tidal currents and suspension during the slack water phase. These muddier sediments cover the ripple-laminated spring-tide structures.

A more directly relevant modern example comes from the high-tide clastic flats of Paso Seco in northern Patagonia (Maisano et al. 2020, 2021). Here, carbonate laminae form continuously within microbial mats, providing analogues for the finely laminated marl packages of Type (1) and stabilising ripple marks to promote their preservation as an analogue for Type (2).

A geobiological model proposed by Maisano et al. (2020, 2021) explains how lenticular and flaser laminations – common in tidal environments – can form and be preserved through microbial influence. In present-day upper sub-tidal and intertidal zones, coarser, organic-rich sediment is supplied primarily from land by rivers. This material is reworked by tides, forming sedimentary structures that are later stabilised by microbial biofilms during periods of calm. Tidal inundation regularly floods the sedimentation basin, creating shallow, stagnant pools that persist for days or weeks. As evaporation progresses, $CaCO_3$ supersaturation is achieved, especially where algal mats restrict permeability and allow gradual water loss. The mats facilitate the precipitation of micritic calcite, which forms a protective layer over the sediment, enhancing its preservation against erosion. This model can be applied to the described case.

Similar, at Schiermonnikoog (North Sea, Netherlands), calcium carbonate precipitation occurs due to mat evaporation and the degradation of cyanobacterial biomass, releasing carbonate into the sediment. This process contributes to the cementation and stabilisation of intertidal clastic sediments (Kremer et al. 2008).

It is also possible that, as in the example from Tessier (1993), a thin diatomaceous film could have formed during emersion periods, aiding in the preservation of fragile sediment and contributing silica for later diagenetic silicification.

These structures have also been documented in ancient environments (e.g., Visser 1980; Alexander et al. 1998; Longhitano et al. 2012) and interpreted as tidal rhythmites (see also Van den Berg et al. 2007; Desjardins et al. 2012). It is important to note that tidal rhythmites are especially common in subtidal settings on the shelf. In such cases, the spring-neap tidal bundling of the rhythmites occurs in 10 s of m of water on the seaward dipping shallow clinothems of muddy subaqueous deltas. The rise and fall of tidal water on the shelf causes hyperpycnal muddy gravity flows on the platform not only to slide down the subaqueous delta foresets but also to be markedly tide modulated, causing the rhythmites. The rhythmites are therefore not directly generated by tidal currents but are tide-modulated gravity flows. The rhythmite gravity flows impart the visibly spectacular repeated thin bed appearance that gradually become finer downslope. The freshwater content trapped in the hyperpycnal flows causes them to be unbioturbated.

Observations from modern settings provide valuable analogues for the interpretation of both sediment types in facies F5, indicating that ripple marks and mud layers may be preserved beneath successive carbonate laminae formed by algal mats. These laminae can repeat cyclically, creating laminated complexes. The structures preserved in the Dynów Marls suggest deposition in an upper tidal or upper intertidal environment, likely within a periodically isolated basin receiving substantial organic input from the mainland.

Additional support of this interpretation is biomarker analyses which confirm also a predominance of terrestrial organic matter (present in mudstone lenses of Type (2) deposit from this facies), accompanied by smaller contributions from algal and bacterial sources and dominance of algal and bacterial input preserved in marly laminae draping ripples. These components were likely deposited in a low-oxygen, but photic zone (Dziadzio et al. 2025).

In summary, facies F5 most likely developed in a tidally influenced environment subject to periodic shifts in depth and energy, ranging from the upper intertidal zone (finely laminated marls, Type 1) to the high-energy portions of the tidal flat (mudstones and laminated sandstones, Type 2).

The depositional setting may have oscillated between an open basin shelf, bay, or lagoon, with varying degrees of biogenic input and also organic matter from the mainland.

Additionally, the cyclicity observed within this facies likely records the alternation between spring tides (facies F5) and neap tides (non-laminated marl sediments of facies F3), with which F5 is interbedded (see also interpretation of facies F6). The alternation of facies B5 and F3 is logical and significant for the interpretation.

In the uppermost part of facies association FIII, Facies F6 is present. A characteristic feature of this facies is the presence of stratification characteristic of mixed high and low-energy environments (wave, flaser and lenticular lamination, horizontal lamination, massive or normal grading). In this facies also bidirectional ripple lamination (Fig. 18) and interfingering of marly laminae within the muddy deposits suggests that the mud drapes covering landward-directed ripple-laminae were deposited during the slack-water period just after the flood half-cycle.

Unrug (1980) interpreted similar sedimentary structures as contourites or tractionites. However, these differ in that they do not create the cyclical, repeated facies successions documented in facies F6 (cf. facies interpretation F1).

Within the horizontally laminated sandstones and mudstones there are several thin intervals with a large accumulation of fish fragments and faecal pellets, also suggesting a high energy environment in which they were fragmented and transported. These are intervals likely document large storms or even tsunamis that influenced this upper level of FAlll. The presence of these storm wave deposits together with the presence of double mud drapes tidal rhythmites and mud drapes within the ripple laminae all provide good evidence that FAlll reflects time intervals of relatively proximal coastal and inner-shelf environments, i.e. levels in the study succession that prograded farthest into the basin.

An important feature described from the F6 facies is the occurrence of lithotype successions (cases (1)–(4), Fig. 21). They indicate changes in the flow regime, probably controlled by tidal processes during the synodal month (see also Brown et al. 1990; Kvale et al. 1995; Coughenour et al. 2009). There is also an increase in the proportion of sandstones and mudstones towards the top of the section (Fig. 4) and cyclic interbedding of facies F6 with facies F3 (Fig. 22).

All of these features indicate that this facies formed in a tidal environment and was recorded as a tidal controlled by the cyclicity of spring and neap tides. The marly intervals of facies F3 that separate them can be interpreted as the effect of both the sedimentation associated with the neap tidal periods that divide the synodal cycles and the periods of cut-off sedimentary basin from the influence of tidal processes and the dominance of deposition by suspension with a simultaneous high degree of evaporation. The basin periodically flooded and during it the deposition of tidal rhythmites and then evaporated, resulting in the deposition of facies F6 and F3, respectively. It cannot be ruled out that such cyclicity is caused by changes in the seasons (see Mosbrugger & Utescher 2005; Mosbrugger et al. 2005).

Biomarkers in F3 indicate an anoxic, hypersaline environment during marl deposition, formed by evaporation during slack water periods. This cyclicity, as well as that within the F5 facies, may reflect periods of connection with the open ocean. Spring-neap tidal indicators reflect periodic fluctuations in water depth, which may have been influenced by storm activity. The abundance of fish remains in these layers may indicate mass mortality events linked to dinoflagellate blooms (their presence has been confirmed by biomarkers).

These blooms produce toxins during periodic population explosions (see, for example, Köster et al. 1998; Dziadzio et al. 2025 and the Britannica entry on dinoflagellates).

No bioturbation was observed within the analysed associations. The absence of bioturbation in dark, organic-rich shales is usually caused by seafloor anoxia (see, for example, MacEachern et al. 2007), although insufficient sediment contrast can also obscure intense bioturbation (see, for example, Dashtgard et al. 2015). In this case, however, it is more likely to be the result of anoxia and periodic hypersalinity, as evidenced by geochemical data (Dziadzio et al. 2025), or extreme ecological conditions, for example changes between freshwater and brackish and hypersaline. This topic is not discussed in this paper.

Implications for the paleogeography of the Menilite Beds

Facies association FAIII is interpreted to show a gradual retrogradation of the shoreline in the basin, indicating an upward deepening trend in the section. It is also important to note that the Magdalena Sandstone (Fig. 4), which overlies the Dynów Marls in stratigraphic continuity, represents a deltaic system with distal and proximal mouth bars (Dziadzio 2015a, b). Tide indicators are also observed in the Magdalena Sandstone (e.g., tidal channels, see Dziadzio 2018).

The succession at section A clearly documents a transition from shallow-water, carbonate-rich facies with tidal influence up to a sand-dominated deltaic facies. Similar facies types occur in the southern part of the Silesian Unit, mainly in the Magdalena Sandstone occurrence zone (cf. Dziadzio et al. 2006, 2016; Dziadzio 2015a, b, 2018), extending over 30 km.

Therefore, the whole sequence of Menilite Beds with Dynów Marls and Magdalena Sandstone was formed by the periodic growth growth of a shelf, which underwent a tectonic collapse after the deposition of these deposits, and there was no cannibalisation of the shallow-water deposits formed at the basin margin (Dziadzio 2015a; Dziadzio et al. 2016) (Fig. 23A and B).

No such trend of changes has been observed in the FAI and FAII associations.

Additionally, these three facies associations can be correlated between each other, despite some facies change (e.g., between section A and B–C).

The diverse facies types of the Dynów Marls between sections A, B, and C suggest that the basin gradually deepened towards the north (Fig. 23A).

The presence of tidal deposits in the southern part of the Silesian Unit, near the margin of the Silesian Cordillera, may be the result of a marine connection that could have been periodically blocked.

The proposed and well-documented shallow-water interpretation of the study area does not preclude the existence of deep-water regions elsewhere in the Paratethys sedimentary basin during the Lower Oligocene.

This interpretation of the Dynów Marls' genesis, integrating multidisciplinary data and facies context, contrasts significantly with previous deep-water submarine fan models (Kotlarczyk 1985; Kotlarczyk & Leśniak 1990; Czapkowicz 2012; Pastucha 2013; Studencka et al. 2016). It is also supported by findings from other parts of the Carpathians, including in the Czech Republic and Austria, although it does not yet resolve the relative depth of the Silesian Basin. Overall, the data from the three sections of the southern Silesian Unit suggest that the Dynów Marls were likely deposited in shallow, (ramp-type) lacustrine or shelf environments with variable salinity, influenced by diverse depositional processes.

Conclusions

The history of research on the Dynów Marls has primarily focused on identifying its components. The conditions of its deposition have not previously been considered and analysed in detail, except for general interpretations (mainly from the Skole Unit) suggesting that the Dynów Marls are the result of carbonate sediment deposition in a submarine fan system (Kotlarczyk & Leśniak 1990; Czapkowicz 2012; Pastucha 2013).

This interpretation differs from others in the same time interval based on detailed sedimentological and geochemical studies from the Czech Republic and Austria, where the

Dynów Marls are interpreted as the result of increased carbonate productivity caused by mass blooms of calcareous nanoplankton and their deposition in the shallow photic zone, accompanied by high organic carbon emplacement in an environment of low salinity or even freshwater and oxygen depletion (Schulz et al. 2004, 2005; Sachsenhofer et al. 2018; Jirman et al. 2019, 2020).

The nanoplankton species, which are the main components of the Dynów Marls, are endemic. Their presence confirms extreme ecological conditions, characterised by very low salinity and/or high nutrient content. Additionally, the Dynów Marls contain uniform and also endemic (euryhaline) types of shallow-water bivalve fauna (Studencka et al. 2016). This deposit is perhaps related to the Solenovian Event in the eastern Paratethys, during which the sedimentary basin became fresh. A similar process of shallowing of the sedimentary basin occurred throughout the Carpathian Arc, where the Menilite Beds and various other accompanying formations, such as the Dynów Marls, were deposited.

Facies analysis of the Dynów Marls, conducted across three stratigraphic sections in the Polish sector of the Outer Carpathians, reveals a shallow-water depositional environment, in contrast to previous work. In the central-eastern part of the Silesian Unit, six sedimentary facies (F1–F6) and three facies associations (FAI–FAIII) were identified.

The integration of these facies interpretations with organic geochemistry results provides a more comprehensive understanding of the sedimentary processes and genesis of the Dynów Marls. The evidence indicates that the marls formed periodically under shallow-water (lacustrine or fresh to brackish water-dominated shelf) conditions and were influenced by tides, waves and a tsunami.

In the southern part of the Silesian Unit, facies F3, F5 and F6 indicate significant tidal influence that waned over time. Bacterial-algal mats occur in facies F5 and the sedimentary structures within facies F6, as well as their arrangement in characteristic facies successions also indicate tidal dynamics. These sequences also reflect cyclicity corresponding to spring and neap tides, and possibly longer periods (synodal months).

FAI association is associated with a diverse paleogeomorphology in a shallow-water sedimentary lake or shelf setting as suggested by previous reconstructed paleogeography (e.g. Rögl 1999), as well as the results of organic geochemistry studies for three different sections (A, B, C).

FAII association indicates shallow water deposition in the lake or tidal shelf that was periodically cut off from the sea. Tsunami-like deposits are recorded in the central part of the Silesian Unit.

FAIII association also reflects shallow water conditions but also records of a gradual deepening of the sedimentary basin confirmed by deposits interpreted as tidal rhythmites with a record of spring and neap tides. This indicates periodic fluctuations in the depth of the sedimentary basin with a tendency towards its deepening where Menilte shale pass up into the deltaic deposits of Magdalena Sandstone (Dziadzio 2015a, b).

The period of sedimentation of the Menilite Beds coincides with major tectonic events in the Carpathians, especially in the Late Eocene, when the Magura Unit was thrust over the Dukla and Silesian units (Roca et al. 2005; Dziadzio et al. 2016). These movements led to the uplift of the Silesian Cordillera (Książkiewicz 1962, 1965; Unrug 1968, 1979), creating the conditions for the development of a tide-influenced shallow water sedimentary basin. In the northern edge of the Silesian Cordillera, a shallow depositional basin formed, where tidal indicators were preserved in the Dynów Marls (Fig. 23A and B). The tides could have been caused by a connection of this part of the Paratethys with the world ocean.

This study presents the first fully documented and continuous stratigraphic record of a Lower Oligocene shallow-water environment in the Silesian Unit. It challenges the long-standing interpretation of deep-marine deposition within a submarine fan context and significantly advances the understanding of paleoenvironmental conditions during the Menilite Beds' sedimentation in the Carpathians.

Understanding the sedimentation conditions of the Dynów Marls requires further stratigraphic, sedimentological and geochemical studies, which the author intends to conduct. The next stage will be to study the succession of the Dynów Marls in the Skole Unit. Initial geochemical studies conducted within this unit (Dziadzio et al. 2025) indicate different sedimentary conditions and a more marine nature of sedimentation. This suggests a complex and diverse sedimentary basin (or basins) system in the Lower Oligocene.

Acknowledgments: This paper is based on the results of statutory work carried out at the Oil and Gas Institute-National Research Institute, Poland, in 2024 (Arch. No: DK 4100-81/24) under the title Sedimentary environments and geochemical parameters of the Lower Oligocene Dynów Marls from the Silesian Unit, Polish Outer Carpathians (in Polish). The author would like to thank the reviewers: Dan Valentin Palcu and František Teťák, for their valuable comments, which substantially improved the manuscript. I would also like to thank Ron Steel for his comments on the manuscript and for the discussions we had in the field, which influenced the final form of the text.

References

Alexander C.R., Davis R.A., Vernon J. & Henry V.J. (Eds.) 1998: Tidalites: processes and products. *SEPM Society for Sedimentary Geology* 61, 1–171.

Allen M.B. & Armstrong H.A. 2008: Arabia–Eurasia collision and the forcing of mid-Cenozoic global cooling. *Palaeogeography, Palaeoclimatology, Palaeoecology* 265, 52–58. https://doi.org/10.1016/j.palaeo.2008.04.021

Arnott R.W. & Southard J.B. 1990: Exploratory flow-duct experiments on combined-flow bed configurations, and some implications for interpreting storm-event stratification. *Journal of Sedimentary Research* 60, 211–219. https://doi.org/10.1306/212F9156-2B24-11D7-8648000102C1865D

Arzani N. 2006: Primary versus diagenetic bedding in the limestone-marl/shale alternations of the epeiric seas, an example from the Lower Lias (early Jurassic) of SW Britain. *Carbonates and Evaporites* 21, 94–109. https//doi.org/10.1007/bf03175469

Bajdek P. & Bienkowska-Wasiluk M. 2020: Deep-sea ecosystem revealed by teleost fish coprolites from the Oligocene of Poland. *Palaeogeography, Palaeoclimatology, Palaeoecology* 540, 109546. https://doi.org/10.1016/j.palaeo.2019.109546

Bathurst R.G.C. 1987: Diagenetically enhanced bedding in argillaceous platform limestones: stratified cementation and selective compaction: *Sedimentology* 34, 749–778. https://doi.org/10.1111/j.1365-3091.1987.tb00801.x

Bellanca A., Claps M., Erba E., Masetti D., Neri R., Premoli Silva I. & Venezia F. 1996: Orbitally induced limestone/marlstone rhythms in the Albian–Cenomanian Cismon section (Venetian region, northern Italy): sedimentology, calcareous and siliceous plankton distribution, elemental and isotope geochemistry. *Palaeogeography, Palaeoclimatology, Palaeoecology* 126, 227–260. https//doi.org/10.1016/S0031-0182(96)00041-7

Berger A., Imbrie J., Hays, J., Kukla G. & Saltzman B. (Eds.) 1984: Milankovitch and Climate: Understanding the Response to Astronomical Forcing. Part 2. *Springer Netherlands, Dordrecht*, 1–895.

Birecki T. 1964: The geological structure of the Bobowa Syncline (in Polish with English summary). *Geological Transactions Polish Academy of Sciences* 21, 1–57.

Bondevik S., Svendsen J.I. & Mangerud J. 1997: Tsunami sedimentary facies deposited by the Storegga tsunami in shallow marine basins and coastal lakes, western Norway. *Sedimentology* 44, 1115–1131. https://doi.org/10.1046/j.1365-3091.1997.d01-63.x

Bottjer D.J., Arthur M.A., Dean W.E., Hattin D.E. & Savrda C.E. 1986: Rhythmic bedding produced in Cretaceous pelagic carbonate environments: sensitive recorders of climatic cycles. *Paleoceanography* 1, 467–481. https://doi.org/10.1029/PA001i004p00467

Bourrouilh-Le Jan F.G, Beck C. & Gorsline D.S. 2007: Catastrophic events (hurricanes, tsunamis and others) and their sedimentary records: introductory notes and new concepts for shallow water deposits. *Sedimentary Geology* 199, 1–11. https://doi.org/10.1016/j.sedgeo.2006.12.007

Brown M.A., Archer A.W. & Kvale E.P. 1990: Neap-spring tidal cyclicity in laminated carbonate channel-fill deposits and its implications: Salem limestone (Mississippian), South-Central Indiana, U.S.A. *Journal of Sedimentary Research* 60, 152–159. https://doi.org/10.1306/212F9133-2B24-11D7-8648000102C1865D

Bustillo M.A., Arribas M.E. & Bustillo M. 2002: Dolomitization and silicification in low-energy lacustrine carbonates (Paleogene, Madrid Basin, Spain). *Sedimentary Geology* 151, 107–126. https//doi.org/10.1016/S0037-0738(01)00234-2

Cattaneo A. & Steel R. J. 2003: Transgressive deposits: a review of their variability. *Earth-Science Reviews* 62, 187–228. https://doi.org/10.1016/S0012-8252(02)00134-4

Coughenour Ch.L., Archer A.W. & Lacovara K.J. 2009: Tides, tidalites, and secular changes in the Earth–Moon system. *Earth-Science Reviews* 97, 59–79. https://doi.org/10.1016/j.earscirev.2009.09.002

Cuadrado D.G. 2020: Geobiological model of ripple genesis and preservation in a heterolithic sedimentary sequence for a supratidal area. *Sedimentology* 67, 2747–2763. https://doi.org/10.1111/sed.12718

Cummings D.I., Dumas S. & Dalrymple R.W. 2009: Fine-grained versus coarse grained wave ripples generated experimentally under large-scale oscillatory flow. *Journal of Sedimentary Research* 79, 83–83. https://doi.org/10.2110/jsr.2009.012

Czapkowicz M. 2012: Facje, profil i geneza utworów ogniwa z Dynowa oraz ogniwa z Rudawki formacji menilitowej (oligocen) na obszarze Błażowa – Siedliska, Pogórze Dynowskie. *Master's thesis, Wydział Geografii i Geologii UJ,* Kraków (in Polish). https://ruj.uj.edu.pl/entities/publication/39099e93-4df6-4382-ade6-cba070876758

Dam G. & Surlyk F. 1993: Cyclic Sedimentation in a Large Wave- and Storm-Dominated Anoxic Lake; Kap Stewart Formation (Rhaetian-Sinemurian), Jameson Land, East Greenland. *Special Publications of the International Association of Sedimentologists* 18, 419–448. https://doi.org/10.1002/9781444304015.ch21

Dashtgard S.E., Snedden J.W. & MacEachern J.A. 2015: Unbioturbated sediments on a muddy shelf: Hypoxia or simply reduced oxygen saturation? *Palaeogeography, Palaeoclimatology, Palaeoecology* 425, 128–138. https://doi.org/10.1016/j.palaeo.2015.02.033

Dawson A.G. & Smith D.E. 2000: The sedimentology of Middle Holocene tsunami facies in northern Sutherland, Scotland, UK. *Marine Geology* 170, 69–79. https://doi.org/10.1016/S0025-3227(00)00066-9

Denommee K.C., Bentley S.J., Harazim D. & Macquaker J.H. 2016: Hydrodynamic controls on muddy sedimentary fabric development on the Southwest Louisiana subaqueous delta. *Marine Geology* 382, 162–175. https://doi.org/10.1016/j.margeo.2016.09.013

Desjardins P.R., Buatois L.A. & Mangano G.M. 2012: Tidal Flats and Subtidal Sand Bodies. In: Knaust D. & Bromley R.G.: Trace Fossils as Indicators of Sedimentary Environments. *Developments in Sedimentology* 64, 529–561. https://doi.org/10.1016/B978-0-444-53813-0.00018-6

Diatom. https://en.wikipedia.org/wiki/Diatom

Dinoflagellate. https://www.britannica.com/science/dinoflagellate

Dott R.H. Jr. & Bourgeois J. 1982: Hummocky stratification: significance of its variable bedding sequences. *Geological Society of America Bulletin* 93, 663–680. https://doi.org/10.1130/0016-7606(1982)93<663:HSSOIV>2.0.CO;2

Duke W.L., Arnott R.W. & Cheel R.J. 1991: Shelf sandstones and hummocky cross stratification; new insights on a stormy debate. *Geology* 19, 625–628. https://doi.org/10.1130/0091-7613(1991)019<0625:SSAHCS>2.3.CO;2

Dziadzio P.S. 2015a: The Lower Oligocene – still deep-water turbidites or rather shallow-marine deposits? In: Leszczyński S., Dziadzio P.S. & Nemec W. (Eds.): Guide to field excursion B8. Some current sedimentological controversies in the Polish Carpathian flysch. Field-trip topic 3: The Lower Oligocene – still deep-water turbidites or rather shallow-marine deposits? *31st IAS Meeting of Sedimentology*, *25–27 June*, 270–279.

Dziadzio P.S. 2015b: The Magdalena Sandstone (Menilite Beds) – an example of shoal-water deltaic sedimentation in the Carpathians. *Nafta-Gaz* 9, 624–631 (in Polish with English summary).

Dziadzio P.S. 2018: Sedimentary environment of the Menilite Beds in the Stróże Thrust Sheet, Silesian Unit, Carpathians. *Nafta-Gaz* 11, 813–820 (in Polish with English summary). https://doi.org/10.18668/NG.2018.11.05

Dziadzio P.S. & Matyasik I. 2021: Sedimentological and geochemical characterisation of the Lower Oligocene Menilite shales from the Magura, Dukla, and Silesian nappes, Polish Outer Carpathians – A new concept. *Marine and Petroleum Geology* 132, 105247. https://doi.org/10.1016/j.marpetgeo.2021.105247

Dziadzio P.S., Borys Z., Kuk S., Masłowski E., Probulski J., Pietrusiak M., Górka A., Moryc J., Baszkiewicz A., Karnkowski P., Karnkowski P.H. & Pietrusiak M. 2006: Hydrocarbon resources of the Polish Outer Carpathians – Reservoir parameters, trap types, and selected hydrocarbon fields: A stratigraphic review. In: Golonka J. & Picha F. J. (Eds.): The Carpathians and Their Foreland: Geology and Hydrocarbon Resources. *American Association of Petroleum Geologists Memoir* 84, 259–291.

Dziadzio P.S., Matyasik I., Garecka M. & Szydło A. 2016: Lower Oligocene Menilite Beds, Polish Outer Carpathians: supposed deep-sea flysch locally reinterpreted as shelfal, based on new sedimentological, micropalaeontological and organic-geochemical data. *Prace Naukowe Instytutu Nafty i Gazu – Państwowego Instytutu Badawczego* 213, 1–120. https://doi.org/10.18668/PN2016.213

Dziadzio P.S., Higgs R. & Drozd A. 2019: Sedimentary environments of the Oligocene Krosno Beds, a new interpretation in the Polish Outer Carpathians. In: Europe Regional Conference 26–27 March 2019. Paratethys Petroleum Systems between Central Europe and the Caspian Region. *Book of Abstracts*, 22–25.

Dziadzio P.S., Matyasik I., Leśniak G. & Bieleń W. 2025: Sedimentary environments and geochemical parameters of the Lower Oligocene Dynów Marls from the Silesian Unit, Polish Outer Carpathians. *Prace Naukowe Instytutu Nafty i Gazu – Państwowego Instytutu Badawczego* 247, 1–132 (in Polish with English abstract). https://doi.org/10.18668/PN2025.247

Ehrenberg S.N., Pickard N.A.H., Henriksen L.B., Svånå T.A., Gutteridge P. & Macdonald D. 2001: A depositional and sequence stratigraphic model for cold-water, spiculitic strata based on the Kapp Starostin Formation (Permian) of Spitsbergen and equivalent deposits from the Barents Sea. *American Association of Petroleum Geologists Bulletin* 85, 2061–2087.

Eicher D.L. & Diner R. 1991: Environmental factors controlling Cretaceous limestonemarl rhythms. In: Einsele G., Ricken W. & Seilacher A. (Eds.): Cycles and Events in Stratigraphy. *Springer-Verlag*, Berlin, 79–93.

Einsele G. 1992: Sedimentary Basins, Evolution, Facies and Sediment Budget. *Springer-Verlag*, Berlin, Heidelberg, 1–628.

Einsele G., Ricken W. & Seilacher A. (Eds.) 1991: Cycles and Events in Stratigraphy. *Springer-Verlag*, Berlin, 1–955.

Fujiwara O., Masuda F., Sakai T., Irizuki T. & Fuse K. 2000: Tsunami deposits in Holocene bay mud in southern Kanto region, Pacific coast of central Japan. *Sedimentary Geology* 135, 219–230. https://doi.org/10.1016/S0037-0738(00)00073-7

Gągała Ł., Vergés J., Saura E., Malata T., Ringenbach J-C., Werner P. & Krzywiec P. 2012: Architecture and orogenic evolution of the northeastern Outer Carpathians from cross-section balancing and forward modeling. *Tectonophysics* 532–535, 223–241. https://doi.org/10.1016/j.tecto.2012.02.014

Gammon P.R., James N.P. & Pisera A. 2000: Eocene spiculites and spongiolites in southwestern Australia: not deep, not polar, but shallow and warm. *Geology* 28, 855–858. https://doi.org/10.1130/0091-7613(2000)28<855:ESASIS>2.0.CO;2

Gates L.M., Jamesa N.P. & Beauchamp B. 2004: A glass ramp: shallow-water Permian spiculitic chert sedimentation, Sverdrup Basin, Arctic Canada. *Sedimentary Geology* 168, 125–147. https://doi.org/10.1016/j.sedgeo.2004.03.008

Gerdes G. 2007: Structures left by modern microbial mats in their host sediments. In: Schieber J., Bose, P.K., Eriksson P.G., Banerjee S., Sarkar S., Altermann W. & Catuneanu O. (Eds.): Atlas of Microbial Mat Features Preserved Within the Siliciclastic Rock Record. *Elsevier*, Amsterdam, 5–38.

Górniak K. 2011: Origin of marls from the Polish Outer Carpathians: lithological and sedimentological aspects. *Mineralogia* 42, 163–297.

Haczewski G. 1989: Coccolith limestone horizon in the Menilite–Krosno Series (Oligocene, Carpathians) – Identification, Correlation and Origin. *Annales Societatis Geologorum Poloniae* 59, 435–523 (in Polish with English summary).

Hallam A. 1986: Origin of minor limestone-shale cycles: climatically induced or diagenetic? *Geology* 14, 609–612. https://doi.org/10.1130/0091-7613(1986)14<609:OOMLCC>2.0.CO;2

Haq B.U. & Ogg J.G. 2024: Retraversing the Highs and Lows of Cenozoic Sea Levels. *The Geological Society of America* 34, 4–11. https://doi.org/10.1130/GSATGG593A.1

Hesse R. 1989: Silica Diagenesis: Origin of Inorganic and Replacement Cherts. *Earth-Science Reviews* 26, 253–284. https://doi.org/10.1016/0012-8252(89)90024-X

Iijima A. 1994: Neogene siliceous, phosphatic and glauconitic sediments of the northwestern Pacific Rim: a comparison with the eastern Pacific Rim. In: Iijima A., Abed A. & Garrison R.E. (Eds.): Siliceous Phosphatic and Glauconitic Sediments of the Tertiary and Mesozoic. *Proceedings of the 29th International Geological Congress*. *VSP*, Utrecht, 5–16.

Jelby M.S., Grundvag S-A., Helland-Hansen W., Olaussen S. & Stemmerik L. 2020: Tempestite facies variability and storm-depositional processes across a wide ramp: Towards a polygenetic model for hummocky cross-stratification. *Sedimentology* 67, 742–781. https://doi.org/10.1111/sed.12671

Jirman P., Geršlová E., Bubík M., Sachsenhofer R.F., Bechtel A. & Więcław D.M. 2019: Depositional environment and hydrocarbon potential of the Oligocene Menilite Formation in the Western Carpathians: A case study from the Loučka section (Czech Republic). *Marine and Petroleum Geology* 107, 334–350. https://doi.org/10.1016/j.marpetgeo.2019.05.034

Jirman P., Geršlová E., Bubík B., Sachsenhofer R.F. & Medvecká L. 2020: Source rock potential of the Oligocene Menilite Formation in the Czech sector of the Subsilesian Unit (Flysch Carpathians) *Geologica Carpathica* 71, 402–417. https://doi.org/10.31577/GeolCarp.71.5.2

Karnkowski P. 1999: Oil and Gas Deposits in Poland. *The Geosynoptics Society GEOS*, Kraków, 1–380.

Köster J., Rospondek M., Schouten S., Kotarba M., Zubrzycki A. & Sinninghe Damsté J.S. 1998: Biomarker geochemistry of a foreland basin: the Oligocene Menilite Formation in the Flysch Carpathians of Southeast Poland. *Organic Geochemistry* 29, 649–669. https://doi.org/10.1016/S0146-6380(98)00182-X

Koszarski L., Sikora W. & Wdowiarz S. 1974: The Flysch Carpathians. Polish Carpathians. In: Maheľ M. (Ed.): Tectonics of Carpathian-Balkan Regions. *Geologický Ustaw Dioniza Štura*, Bratislava, 180–197.

Kotlarczyk J. 1966: Poziom diatomitowy z warstw krośnieńskich na tle budowy geologicznej jednostki skolskiej w Karpatach polskich. Diatomite Horizon of the Krosno Beds in the Skole nappe, Polish Carpathians. *Studia Geologica Polonica* 19, 1–129 (in Polish with English summary).

Kotlarczyk J. 1985: An outline of the stratigraphy of marginal tectonic units of the Carpathian orogen the Rzeszów–Przemyśl area. Second day: Baranów–Rzeszów–Błażowa–Przemyśl. Stop 10: The Dynów Marls, Łysa Góra, Straszydle. In: Kotlarczyk J. (Ed.): Geotraverse Kraków–Baranów–Rzeszów–Przemyśl–Ustrzyki Dolne–Komańcza-Dukla. Guide to excursion 4, Carpatho–Balcan Geological Association, XIII Congress. *Geological Institute*, Kraków, 39–64, 100–102.

Kotlarczyk J. & Kaczmarska I. 1987: Two diatom horizon in the Oligocene and (?) Lower Miocene of the Polish Outer Carpathians. *Annales Societatis Geologorum Poloniae* 57, 143–188.

Kotlarczyk J. & Lesniak T. 1990: Lower part of the Menilite Formation and related Futoma diatomite member in the Skole unit of the Polish Carpathians. *Wydawnictwo Akademii Górniczo–Hutniczej*, Kraków, 1–74 (in Polish with English summary).

Kotlarczyk J., Brożek M. & Michalski M. 1986: Diatomity polskich Karpat – wykształcenie, jakość, przeróbka i zastosowanie. *Gospodarka Surowcami Mineralnymi* 2, 3–4 (in Polish).

Kotlarczyk J., Jerzmańska A., Świdnicka E. & Wiszniowska T. 2006: A frame work of ichthyofaunal ecostratigraphy of the Oligocene–Early Miocene strata of the Polish Outer Carpathian basin. *Annales Societatis Geologorum Poloniae* 76, 1–111.

Kremer B., Kazmierczak J. & Stal J. 2008: Calcium carbonate precipitation in cyanobacterial mats from sandy tidal flats of the North Sea. *Geobiology* 6, 46–56. https://doi.org/10.1111/j.1472-4669.2007.00128.x

Krhovský J. 1981: Stratigraphy and palaeoecology of the Menilite Formation of the Ždánice unit and of the diatomites of the Pouzdřany unit (the western Carpathians, Czechoslovakia). *Zemný Plyn a Nafta* 26, 45–62 (in Czech with English summary).

Krhovský J., Adamová J., Hladiková J. & Maslowská H. 1992: Paleoenvironmental changes across the Eocene/Oligocene boundary in the Ždánice and Pouzdrany units (western Carpathians, Czechoslovakia): the long-term trend and orbitality forced changes in nannofossils as sem blages. *Zemní Plyn a Nafta* 14b, 105–187.

Krhovský J., Rögl F. & Hamršmid B. 2001: Stratigraphic correlation of the Late Eocene to Early Miocene of the Waschberg Unit (Lower Austria) with Ždanice and Pouzdrany Units (South Moravia). *Schriftenreihe der Erdwissenschaftlichten Kommissionen* 14, 225–254.

Książkiewicz M. (Ed.) 1962: Atlas geologiczny Polski. Zagadnienia stratygraficzno-facjalne. Z. 13, Kreda i starszy trzeciorzęd w polskich Karpatach zewnętrznych. *Instytut Geologiczny*, Warszawa (in Polish).

Książkiewicz M. 1965: Les cordilleres dans les mers cretacees et paleogenes des Carpates du Nord. *Bulletin de la Société géologique de France* S7-VII, 443–455. https://doi.org/10.2113/gssgfbull.S7-VII.3.443

Książkiewicz M. 1975: Bathymetry of Carpathian flysch basin. *Acta Geologica Polonica* 25, 309–367.

Kvale E.P., Cutright J., Bilodeau D., Archer A.W., Johnson H.R. & Pickett B. 1995: Analysis of modern tides and implications for ancient tidalites. *Continental Shelf Research* 15, 1921–1943. https://doi.org/10.1016/0278-4343(95)00001-H

Lazar R.O., Bohacs K.M., Schieber J., Macquaker J.H.S. & Demko T.M. 2012: Mudstone Primer: Lithofacies variations, diagnostic criteria, and sedimentologic–stratigraphic implications at lamina to bedset scale. *SEPM Concepts in Sedimentology and Paleontology* 12, 1–199. https://doi.org/10.2110/sepmcsp.12.

Lazar O.R., Bohacs K.M., Macquaker J.H.S., Schieber J. & Demko T.M. 2015: Capturing key attributes of fine-grained sedimentary rocks in outcrops, cores, and thin sections: Nomenclature and description guidelines: *Journal of Sedimentary Research* 85, 230–246. https://doi.org/10.2110/jsr.2015.11

Li J., Cai Z., Chen H., Cong F., Wang L., Wei Q. & Luo Y. 2018: Influence of differential diagenesis on primary depositional signals in limestone-marl alternations: An example from Middle Permian marine successions, South China. *Palaeogeography, Palaeoclimatology, Palaeoecology* 495, 139–151. https://doi.org/10.1016/j.palaeo.2018.01.002

Longhitano S.G., Mellere D., Steel R.J. & Ainsworth B.R. 2012: Tidal depositional systems in the rock record: a review and new insights. *Sedimentary Geology* 279, 2–22. https://doi.org/10.1016/j.sedgeo.2012.03.024

MacEachern J.A., Pemberton S.G., Bann K.L. & Gingras M.K. 2007: Departures from the Archetypal Ichnofacies: EffectIve recognition of physico-chemical stresses In the rock record. In: MacEachern J.A., Bann K.L., Gingras M.K. & Pemberton S.G. (Eds.): Applied Ichnology *SEPM Short Course Notes* 52 (CD Edition), 65–95.

Maisano L., Quijada I.E., Cuadrado D.G., Perillo V.L., Pan J. & Martinez A.M. 2020: Carbonate laminae recorded in a siliciclastic tidal flat colonized by microbial mats. *Sedimentary Geology* 405, 105702. https://doi.org/10.1016/j.sedgeo.2020.105702

Maisano L., Quijada I.E., Perillo V.L., Cuadrado D.G., Raniolo A.L. & Gómez E.A. 2021: Contribution of carbonate precipitation to the preservation of ripples in siliciclastic sediments colonized by microorganisms. *Latin American Journal of Sedimentology and Basin Analysis* 28, 121–132.

Malata T. & Poprawa P. 2006: Evolution of the Skole subbasin. In: Oszczypko N., Uchman A. & Malata E. (Eds.): Palaeotectonic Evolution of the Outer Carpathian and Pieniny Klippen Belt Basins. *Instytut Nauk Geologicznych Uniwersytetu Jagiellońskiego*, Kraków, 103–110 (in Polish).

Miller K.G., Browning J.V., Schmelz W.J., Kopp R.E., Mountain G.S. & Wright J.D. 2020: Cenozoic sea-level and cryospheric evolution from deep-sea geochemical and continental margin records. *Science Advances* 6, eaaz1346.

Morales J.A. 2022: Coastal Geology. Chemical Processes and Sediments on the Coast. Textbooks in Earth Sciences, Geography and Environment. *Springer*, 1–463 (eBook). https://doi.org/10.1007/978-3-030-96121-3

Morales J.A., Gutiérrez-Mas J.M., Borrego J. & Rodríguez-Ramírez A. 2011: Sedimentary characteristics of the Holocene tsunamigenic deposits in the coastal systems of the Cadiz Gulf (Spain). In: Mörner N.-A. (Ed.): The Tsunami threat: research and technology. *InTech*, Rijeka, 237–258.

Morsilli M. & Pomar L. 2012: Internal waves vs. surface storm waves: a review on the origin of hummocky cross-stratification. *Terra Nova* 24, 273–282. https://doi.org/10.1111/j.1365-3121.2012.01070.x

Mosbrugger V. & Utescher T. 2005: Cenozoic continental climatic evolution of Central Europe. *Proceedings of the National Academy of Sciences of the United States of America* Supplement, 102, 14964–14969. https://doi.org/10.1073/pnas.0505267102

Mosbrugger V., Utescher T. & Dilcher D. 2005: Cenozoic palaeoclimate reconstructions from 35 sites in Central Europe. *PANGAEA Data Publisher for Earth & Environmental Science*. https://doi.org/10.1073/pnas.050526710

Myrow P.M. 2005: Storms and storm deposits. In: Selley R.C., Cocks R. & Pilmer I. (Eds.): Encyclopedia of Geology. *Elsevier Limited*, Oxford, 580–587.

Myrow P.M. & Southard J.B. 1996: Tempestite deposition. *Journal of Sedimentary Research* 66, 875–887. https://doi.org/10.1306/D426842D-2B26-11D7-8648000102C1865D

Nemčok M., Nemčok J., Wojtaszek M., Ludhová L., Klecker R.A., Sercombe W.J., Coward M.P. & Keith J.F jr. 2000: Results of 2D balancing along 20° and 21°30' longitude and pseudo-3D in the Smilno tectonic window: implications for shortening mechanisms of West Carpathians accretionary wedge. *Geologica Carpathica* 51, 281–300.

Newell R.C. 1979: Biology of Intertidal Animals. *Marine Ecological Surveys Ltd*., Faversham, Kent, 1–781.

Nohl T., Jarochowska E. & Munnecke A. 2019: Revealing the genesis of limestone-marl alternations: A Taphonomic approach. *Palaios* 34, 15–31. https://doi.org/10.2110/palo.2018.062

Pastucha M. 2013: Facje, profil i geneza utworów ogniwa z Dynowa oraz ogniwa z Rudawki formacji menilitowej (oligocen) na obszarze Ustrzyki Dolne-Krościenko, Karpaty. *Master's thesis*, *Wydział Geografii i Geologii UJ*, Kraków (in Polish). https://ruj.uj.edu.pl/entities/publication/4ce391e0-b0ae-4dae-be75-bd6f2d8d2f43\

Patruno S., Hampson G.J., Jackson Ch.A.-L. & Dreyer T. 2015: Clinoform geometry, geomorphology, facies character and stratigraphic architecture of a sand-rich subaqueous delta: Jurassic Sognefjord Formation, offshore Norway. *Sedimentology* 62, 350–388. https://doi.org/10.1111/sed.12153

Pisciotto K.A. & Garrison R.E. 1981: Lithofacies and Depositional Environments of the Montery Formation, California. In: Garrison R.E. & Douglas R.G. (Eds.): The Monterey Formation and Related Siliceous Rocks of California. *SEPM Research Symposium Society for Sedimentary Geology*, Tulsa, 97–122.

Pisera A. 1991: Upper Jurassic sponge megafacies in Spain: preliminary report. In: Reitner J. & Keupp H. (Eds.): Fossil and Recent Sponges. *Springer-Verlag*, Berlin, 486–497.

Pittet B., Strasser A. & Mattioli E. 2000: Depositional sequences in deep-shelf environments: a response to sea-level changes and shallow-platform carbonate productivity (Oxfordian, Germany and Spain). *Journal of Sedimentary Research* 70, 392–407. https://doi.org/10.1306/2DC40918-0E47-11D7-8643000102C1865D

Popov S.V. & Studencka B. 2015: Brackish-water Solenovian mollusks from the lower Oligocene of the Polish Carpathians. *Paleontological Journal* 49, 342–355.

Pupp M., Bechtel A., Gratzer R., Heinrich M., Kozak S., Lipiarski P. & Sachsenhofer R.F. 2018: Depositional environment and petroleum potential of Oligocene rocks in the Waschberg Zone (Austria). *Geologica Carpathica* 69, 410–436. https://doi.org/10.1515/geoca-2018-0024

Roca E., Bessereau G., Jawor E., Kotarba M. & Roure F. 1995: Pre-neogene evolution of the western Carpathians: constraints from the bochnia-tatra mountains section (Polish Western Carpathians). *Tectonics* 14, 855–873. https://doi.org/10.1029/95TC00828

Rögl F. 1999: Mediterranean and Paratethys. Facts and hypotheses of an Oligocene to Miocene paleogeography (short overview). *Geologica Carpathica* 50, 339–349.

Rossi V.M. & Steel R.J. 2016: The role of tidal, wave and river currents in the evolution of mixed-energy deltas: Example from the Lajas Formation (Argentina). *Sedimentology* 63, 824–864. https://doi.org/10.1111/sed.12240

Rossi V.M., Perillo M.M., Steel R.J. & Olariu C. 2017: Quantifying mixed-process variability in shallow-marine depositional systems: what are sedimentary structures really telling us? *Journal of Sedimentary Research* 2017, 1–15. https://doi.org/10.2110/jsr.2017.49

Sachsenhofer R.F., Popov S.V., Ćorić S., Mayer J., Misch D., Morton M.T., Pupp M., Rauball J. & Tari G. 2018: Paratethyan petroleum source rocks: an overview. *Journal of Petroleum Geology* 41, 219–246. https://doi.org/10.1111/jpg.12702

Schulz H.M., Bechtel A., Rainer T, Sachsenhofer R.F. & Struck U. 2004: Paleoceanography of the western Central Paratethys during nannoplankton zone NP 23. *Geologica Carpathica* 55, 311–323.

Schulz H.M., Bechtel A. & Sachsenhofer R.F. 2005: The birth of the Paratethys during the early Oligocene: from tethys to an ancient Black Sea analogue? *Global and Planetary Change* 49, 163–176. https://doi.org/10.1016/j.gloplacha.2005.07.001

Ślączka A. & Kaminski M. A. 1998: A Guidebook to Excursions in the Polish Flysch Carpathians. Field Trips for Geoscientists. *Grzybowski Foundation Special Publications* 6, 1–173.

Studencka B., Sergey V. Popov V.S., Bieńkowska-Wasiluk M. & Wasiluk R. 2016: Oligocene bivalve faunas from the Silesian Nappe, Polish Outer Carpathians: evidence of the early history of the Paratethys. *Geological Quarterly* 60, 317–340. https://doi.org/10.7306/gq.1296

Sugitani K., Yamamoto K., Adachi M., Kawabe I. & Sugisaki R. 1998: Archean cherts derived from chemical, biogenic and clastic sedimentation in a shallow restricted basin – examples from the Gorge Creek Group in the Pilbara Block. *Sedimentology* 45, 1045–1062. https://doi.org/10.1046/j.1365-3091.1998.00198.x

Steel R., Osman A., Rossi V., M., Alabdullatif J., Olariu C., Peng Y. & Rey F. 2024: Subaqueous deltas in the stratigraphic record: Catching up with the marine geologists. *Earth-Science Reviews* 256, 104879. https://doi.org/10.1016/j.earscirev.2024.104879

Švábenická L., Bubík M. & Stráník Z. 2007: Biostratigraphy and palaeoenvironmental changes on the transition from the menilite to Krosno lithofacies (western Carpathians, Czech Republic). *Geologica Carpathica* 58, 237–262.

Świdziński H. 1947: Słownik stratygraficzny północnych Karpat fliszowych. *Biuletyn Państwowego Instytutu Geologicznego* 37, 1–124 (in Polish).

Szymakowska F. 1979: Budowa geologiczna południowego skrzydła fałdu Gorlic między Gorlicami a Krygiem (Karpaty Środkowe). *Annales de la Societé géologique de Pologne* 49, 85–103 (in Polish).

Tessier B. 1993: Upper intertidal rhythmites in the Mont-Saint-Michel Bay (NW France): Perspectives for paleoreconstruction *Marine Geology* 110, 355–367. https://doi.org/10.1016/0025-3227(93)90093-B

Tessier B., Archer A.W., Lanier W.P. & Feldman H.R. 1995: Comparison of Ancient Tidal Rhythmites (Carboniferous of Kansas and Indiana, USA) with Modern Analogues (the Bay of Mont-Saint-Michel, France). *Special Publications of the International Association of Sedimentologists* 24, 259–271. https://doi.org/10.1002/9781444304138.ch17

Tinterri R. 2011: Combined flow sedimentary structures and the genetic link between sigmoidal- and hummocky-cross stratification. *GeoActa* 10, 43–85.

Tucker M.E. 1991: Sedimentary Petrology. An Introduction to the Orgin of Sedimentary Rocks, 2nd edn. *Blackwell Scientific Publications*, Oxford, 1–260.

Unrug R. 1968: The Silesian cordilliera as the source of clastic material of the Flysch sandstone of the Beskid Śląski and Beskid Wysoki ranges (Polish Western Carpathians). *Annales Societatis Geologorum Poloniae* 38, 81–166.

Unrug R. 1979: Palinspastic reconstruction of the Carpathian Arc before the Neogene tectogenesis. *Annales Societatis Geologorum Poloniae* 49, 3–21.

Unrug R. 1980: Ancient contourites in the Menilite Beds (Oligocene) of the Carpathian Flysch, Poland. Annales *Societatis Geologorum Poloniae* 50, 175–182.

Van den Berg J.H., Boersma J.R. & Van Gelder A. 2007: Diagnostic sedimentary structures of the fluvial-tidal transition zone – Evidence from deposits of the Rhine and Meuse. *Netherlands Journal of Geosciences* 86.3, 287–306.

Visser M.J. 1980: Neap-spring cycles reflected in Holocene subtidal large-scale bedform deposits: A preliminary note. *Geology* 8, 543–546. https://doi.org/10.1130/0091-7613(1980)8%3C543:NCRIHS%3E2.0.CO;2

Walker L.J., Wilkinson B.H. & Ivany L.C. 2002: Continental drift and Phanerozoic carbonate accumulation in shallow-shelf and deep-marine settings. *Journal of Geology* 110, 75–87.

Wasiluk R. 2016: Objaśnienia do szczegółowej mapy geologicznej Polski, Arkusz Krosno, 1:50,000. *Ministerstwo Środowiska*, Warszawa.

Westphal H. 2006: Limestone-marl alternations as environmental archives and the role of early diagenesis: a critical review. *International Journal of Earth Sciences* 95, 947–961. https://doi.org/10.1007/s00531-006-0084-8

Westphal H., Munnecke A., Bo Hm F. & Bornholdt S. 2008: Limestone-marl alternations in epeiric sea settings—witnesses of environmental changes, or of rhythmic diagenesis? In: Holmden C. & Pratt B.R. (Eds.): Dynamics of Epeiric Seas. *Sedimentological, Paleontological and Geochemical Perspectives: Geological Association of Canada Special Paper* 48, 389–406.

Whelan F. & Kelletat D. 2005: Boulder deposits on the southern Spanish Atlantic coast: possible evidence for the 1755 AD Lisbon tsunami? *Science of Tsunami Hazards* 23, 25–38.

Yang B., Dalrymple R.W. & Chun S. 2006: The significance of hummocky cross-stratification (HCS) wavelengths; evidence from an open-coast tidal flat, South Korea. *Journal Sedimentary Research* 76, 2–8. https://doi.org/10.2110/jsr.2006.01

Zavala C., Arcuri M., Di Meglio M.D., Zorzana A. & Otharan G. 2021: Deltas, a new classification expanding Bates concepts. *Journal of Palaeogeography* 10, 23. https://doi.org/10.1186/s42501-021-00098-w